Role of the class I PI3K p110β and PtdIns(3,4,5)P_3 in rRNA transcription in the nucleolus

Victoria Smith Arnesen

This thesis is submitted in partial fulfilment of the

requirements for the degree of Master of Science

Department of Biological Sciences

Faculty of Mathematics and Natural Sciences

University of Bergen

June 2018

Acknowledgements

The work presented in this thesis was carried out at the Department of Biological Sciences, University of Bergen, in the period August 2017 to May 2018.

First, I would like to thank my amazing supervisor Aurélia E. Lewis. Thank you so much for all your guidance and help throughout this past year. Your ability to switch gears and concentrate on my problem as I knock on your door never ceases to amaze me. Your cheery and positive attitude always made me feel welcome, and I never hesitated to come to you if I had questions or wanted a chat. The devotion and enthusiasm you have for lipids and the world of science is truly inspiring.

I also give my sincere thanks to my co-supervisor Fatemeh Mazloumi Gavgani. Through the first semester of working on my project you taught me everything I now know. Your careful and calculated ways of performing experiments has taught me to respect the reagents I work with, and always check that the bottle of chloroform is shut. It's definitely shut, right? Jokes aside, you really have been a wonderful teacher, and I appreciate our chats about everything, small and large, lab-related and not!

I would also like to extend my thanks to Diana C. Turcu. Whenever I had a silly question, you would always be there, ready to give an answer, and I honestly appreciate it. You are a treasure to have in the lab! Thank you to Joakim Brunet, for helping me setting up the qPCR program… every single time I used it! I would like to thank Olena Dobrovolska for doing the preliminary NMR experiments. I hope the continued work brings exciting results! Thanks to Marc Niere for dropping in and giving helpful hints and terrible jokes! Thank you to the rest of the NucReg team, for providing a wonderful work-environment!

My sincere gratitude goes to Camila, my fellow sufferer and dearest friend. Your calls to ensure I was working steadily and making progress really pushed me to work harder and do better. I appreciate the times we've spent together over the past 2 years, especially the past few months. It's been a long journey, and as happy as I am to soon be done, I will miss this time with you!

I would also like to thank my family and friends, and especially my husband-to-be Hasan. Writing together and supporting each other has really given me the energy and will to see this through. You are my rock, and I love you so very much!

Table of Contents

Selected abbreviations

PI3K	Phosphoinositide 3-Kinase
PtdIns	Phosphatidyl inositol
PI	Phosphoinositide
PPIn	Polyphosphoinositide
p110β	Class I PI3K isoform β
PIP3	PtdIns(3,4,5)P_3
Akt	Protein kinase B
PTEN	Phosphatase and tensin homolog
Pol I	RNA polymerase I
rRNA	Ribosomal RNA
ETS	External transcribed spacer
EC	Endometrial cancer
NLS	Nuclear localisation signal
KR-motif	Polybasic lysine/arginine-rich motif
PARP1	Poly(ADP-ribose) polymerase I
UBF	Upstream binding transcription factor I

1 Abstract

The phosphoinositide 3-kinase (PI3K) signalling pathway is one of the most altered pathways in human cancer. It is a complex pathway, when considering that ubiquitously expressed isoforms regulate different routes with their own cellular outcomes. The majority of research has been focused on the PI3K p110α isoform, due to frequent findings of mutations in different human cancers. The PI3K p110β isoform has received less attention, however it has been found to be tumorigenic when overexpressed in its wild-type form, which has been linked to its lipid kinase activity. Our group has focused on p110β and shown that the mRNA for the p110β-coding gene *PIK3CB* are elevated in endometrial cancer cell lines. Also, our group has demonstrated that the nuclear levels of PtdIns(3,4,5)P_3 (PIP3), the lipid product of p110β, is high in the endometrial cancer cell line RL95-2. Both p110β and PIP3 have been found to localise in the nucleus and nucleolus of some cell lines, though their role in the nucleolus is still unknown.

During this study, p110β and its lipid product PIP3 was confirmed to localise within the nucleoli of RL95-2 cells. To determine what the purpose of p110β and PIP3 is within nucleoli and ribosomal biogenesis, p110β was inhibited by Kin193, a specific p110β inhibitor. The results show a decrease in 47S rRNA transcription, the initial ribosomal transcript. Labelling nascent rRNA with and without Kin193 showed that inhibiting p110β indeed led to decreased rRNA fluorescent signal in human cells. These findings further validate Kin193 as a potential anti-cancer drug in patients with endometrial cancer. The experiments were also performed on two mouse cell lines, one p110β wild type (WT) and a p110β catalytic mutant (KI), though there were no significant differences between them.

For PIP3 to function as a signalling lipid, it must bind and recruit proteins. During a PIP3 lipid pull-down from the nuclei of HeLa cells, our group found a cohort of potential PIP3 effector proteins. One of these was poly(ADP-ribose) polymerase I (PARP1), which is involved in single stranded DNA break repair, amongst other roles. PARP1 has also been found to localise in the nucleolus, along with PIP3, and PTEN-deficient endometrial cancer cells have been shown to be sensitised to PARP1 inhibition. PARP1 contains multiple KR-motifs, which are known to bind PIP3. The results show that fragments 1, 2 and 3 bind a variety of lipids, including PIP3. Fragment 3, which contains a KR-motif, was also analysed in NMR spectroscopy, where the KR-motif was confirmed to be part of PIP3 interaction.

2 Introduction

2.1 Phosphoinositide 3-Kinase signalling

The phosphoinositide 3-Kinase (PI3K) signalling pathway has been the subject of a lot of attention in recent years due to its involvement in a variety of cellular functions and human diseases like cancer and diabetes mellitus type 2. The range of lipid-protein interaction managed by PI3Ks has raised an assortment of questions regarding their effects on the cell.

2.1.1 Polyphosphoinositides

Polyphosphoinositides (PPIn) are phosphorylated derivatives of the lipid phosphatidylinositol (PtdIns), which are involved in a wide array of cell functions. These include protein interaction, gene expression, cell cycle progression and signal transduction, to name a few (Di Paolo and De Camilli, 2006). PtdIns is a glycerophospholipid consisting of a glycerol backbone connected to an inositol headgroup on the 1' OH group through a phosphodiester bond, along with two hydrophobic acyl chains, connected via ester bonds (**Figure 2.1**). The inositol ring can be reversely phosphorylated on the 3', 4' and 5' positions, resulting in one of seven different PPIns. These seven variants are divided into one tri-phosphorylated (PtdIns(3,4,5)P_3), three di-phosphorylated (PtdIns(3,4)P_2, PtdIns(3,5)P_2 and PtdIns(4,5)P_2) and three mono-phosphorylated PPIn (PtdIns3*P*, PtdIns4*P* and PtdIns5*P*), with the majority PPIn being PtdIns4*P* and PtdIns(4,5)P_2 in mammalian cells. PPIn are fairly low-abundance molecules, comprising only 1% of the total lipid content in the cell (Viaud *et al.*, 2016). Using the fatty acyl chains, PPIn are known to anchor themselves to membranes through hydrophobic interactions on the plasma and intra-cellular membranes (Van Meer *et al.*, 2008). The inositol headgroup is then exposed to the solvent, allowing it to interact with proteins. Depending on the proteins and cellular processes involved, this can elicit a variety of results.

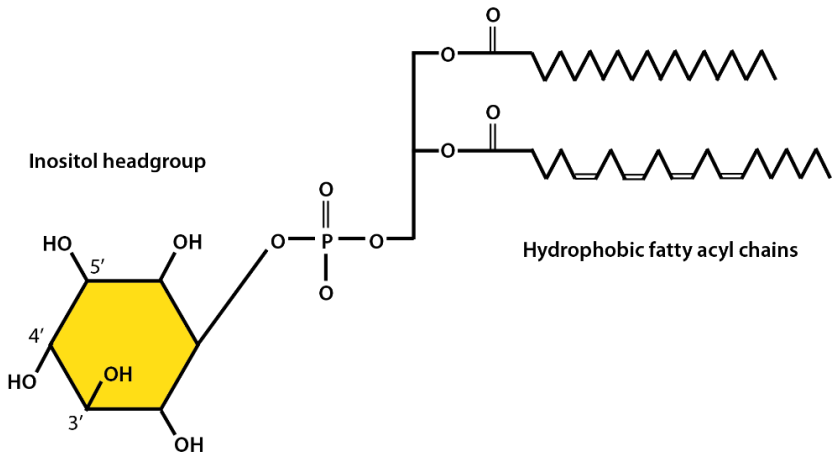

Figure 2.1. Phosphatidylinositol structure diagram. The hydrophobic fatty acid chains shown (C18:0/C20:4) are attached to the glycerol backbone via ester bonds, which is linked to the inositol headgroup through a phosphodiester bond.

PPIn act as signal transducers by recruiting proteins with phosphoinositide (PI)-binding domains to specific sub-cellular membranes. These domains are usually multi-domain proteins involved in regulating cellular function, and include the FYVE (named after the four first proteins in which it was identified: Fab1p, YOTB, Vac1p and EA1), pleckstrin homology (PH), Phox homology, epsin amino-terminal homology, and radixin domains, to name a few (Lemmon, 2003). Of these, only the PH domain has been shown to bind PtdIns(3,4,5)P_3 (Lemmon, 2003). However, in addition to these structured PI-domains, unstructured PI-binding motifs also exist, which are characterised by their sequence and charge, rather than a defined structural domain. These are short stretches of basic amino acids, often denoted as lysine/arginine-rich patches or KR-motifs (K/R-($X_{n=3-7}$)-K/R-X-K/R-K/R), and have been shown to have PI-binding properties (Martin, 1998). Using specific electrostatic interactions provided by this sequence, many actin regulatory proteins are able to bind PPIn (Zhang *et al.*, 2012). Also, Kumar *et al*. demonstrated that the first basic residue is especially important, as a point mutation in this residue in a KR-motif in the protein villin (Arg138) to alanine led to decreased binding to PtdIns(4,5)P_2 (Kumar *et al.*, 2004).

2.1.2 The PI3K/Akt/mTOR pathway

The family in charge of phosphorylating the 3’ OH of the inositol head group of PtdIns is called the phosphoinositide 3-kinase (PI3K) family. The PI3K family is divided into 3 main classes; I, II and III, and are responsible for generating PtdIns(3)*P*, PtdIns(3,4)P_2 and PtdIns(3,4,5)P_3. Class I PI3Ks are heterodimers consisting of a catalytic subunit, either p110α, p110β, p110γ or p110δ, and a regulatory subunit of p85α, p85β, p55, p101 or p87 (Vanhaesebroeck and

Waterfield, 1999). Class II PI3Ks are monomers and are responsible for producing PtdIns3*P*, though they have been shown to generate PtdIns(3,4)P_2 *in vitro*, and possibly also *in vivo* (Posor *et al.*, 2013). They consist of three isoforms in mammalian cells; PI3K-C2α, PI3K-C2β and PI3K-C2γ, and their preferred substrate is PtdIns (Falasca and Maffucci, 2007). The only known Class III PI3K, vacuolar protein sorting 34 (Vps34), is bound to its adaptor protein Vps15, and produces PtdIns3*P* (Stack *et al.*, 1995).

The emphasis in this thesis was on Class I PI3Ks, and so further discussion will be focused on this class. In Class I PI3Ks, all four p110 isoforms are transcribed from separate genes, and thus can be regulated independently (Sasaki *et al.*, 2009). The p110 subunit consists of an N-terminal p85 binding domain, a Ras-binding domain, a C2 domain, a helical domain, and a C-terminal catalytic domain. The p85 regulatory subunit's core structure contains a coiled coil p110-binding domain surrounded by two Src homology domains (Vadas *et al.*, 2011). They are activated through either a receptor tyrosine kinase (for p110α, p110β and p110δ) or a G-protein coupled receptor (for p110β and p110γ) (Jean and Kiger, 2014).

The substrate of class I PI3Ks is PtdIns(4,5)P_2 *in vivo*, resulting in the tri-phosphorylated PtdIns(3,4,5)P_3 (PIP3). Under inactive conditions, the regulatory p85 subunit inhibits the catalytic p110 subunit through interaction. Upon binding of p85 to the receptor, the catalytic subunit is activated, and the p110 subunit generates PIP3. PIP3 is a crucial signalling molecule, and the PI3K/Akt/mTOR signalling pathway is initiated by the binding of PIP3 to Akt, through a pleckstrin homology (PH) domain. Akt, also known as protein kinase B, becomes active by PIP3 binding and phosphorylation on specific amino acid residues, leading to downstream effects including cell differentiation, cell growth, proliferation and cell survival. The activating phosphorylations of Akt is carried out by two protein kinases; phosphoinositide-dependent protein kinase 1 (PDK1) and mammalian target of rapamycin (mTOR) complex 2, which phosphorylate Akt on Thr308 and Ser473 respectively (Sarbassov *et al.*, 2005).

Due to the capabilities of PPIn as signalling molecules, they are under tight regulation in the cell, and the levels of 3'-phosphorylated PPIn are controlled exclusively by different kinases and phosphatases. The tumour suppressor phosphatase and tensin homolog (PTEN) is an antagonist of the PI3K pathway, in that it dephosphorylates PtdIns(3,4,5)P_3 to PtdIns(4,5)P_2, thus negatively regulating the pathway (Maehama and Dixon, 1998). PTEN is regarded as a tumour suppressor due to frequent findings of mutations that lead to loss-of-function in certain

human cancers (Wang and Jiang, 2008). Other PIP3 phosphatases include 5'-phosphatases, like SH2-containing inositol polyphosphatase type 2 (SHIP2) and inositol polyphosphate 5-phosphatase (INPP5) (Sasaki *et al.*, 2009), though their role in terminating the PI3K pathway is still unclear.

Class I PI3Ks are further divided into classes IA and IB, where class IA consists of a p85 (α or β), p55α, p50α or p55γ subunit and a p110 (α, β and δ) catalytic subunit. Class IB only consists of the catalytic p110γ subunit, and the p101 or p84 (also known as p87) regulatory subunit (Okkenhaug, 2013). While isoforms p110δ and p110γ are restricted to immune cells, p110α and p110β are ubiquitously expressed (Vanhaesebroeck and Waterfield, 1999). p110α and β share the same substrate, PtdIns(4,5)P_2, have high sequence homology, similar catalytic property, can have the same mode of activation, and are both embryonically lethal when knocked out (Bi et al., 1999; Bi et al., 2002). Based on this information, it would appear redundant to have both these isoforms present at any given time. However, upon closer inspection, it becomes clear that they serve dissimilar cellular roles, possibly emanating from different sub-compartments of the cell (Benistant et al., 2000; Marques et al., 2009). Indeed, a key difference is their sub-cellular localization; both isoforms are present in the cytoplasm, however p110β is also found in the chromatin enriched fractions of the nucleus, and in nucleoli (*Karlsson et al*., 2016; Kumar et al., 2011). Another small, but significant difference lies in the presence or absence of a nuclear localisation signal (NLS) motif (see **Figure 2.2)**. Though their p85- and Ras-binding domains, as well as the helical and catalytic domains are more or less equal in size and localisation in the sequence, the PI3K-C2 domain in p110β contains a NLS motif that is absent from p110α (Kumar *et al.*, 2011). In the same study, Kumar *et al*. found that there is a nuclear export sequence (NES) within the p85β regulatory subunit, allowing p85β/p110β entry to, and exit from, the nucleus.

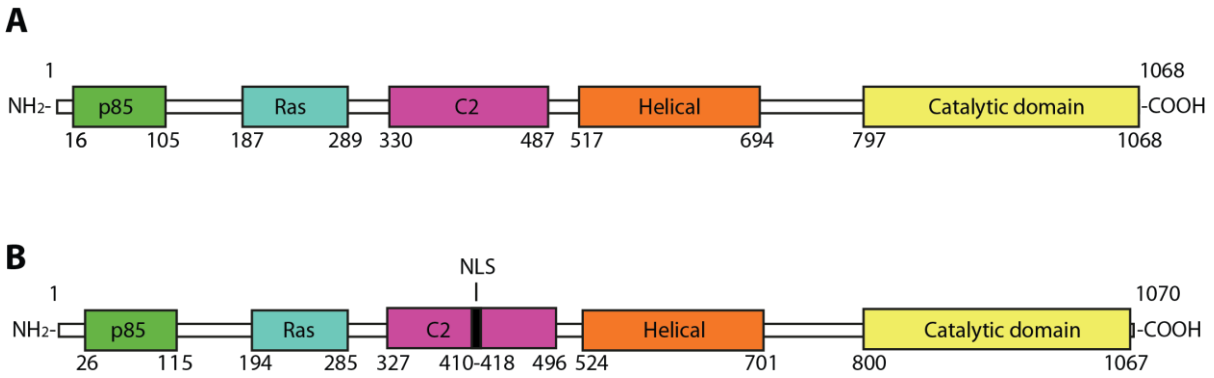

Figure 2.2. Differences in domain structure for p110α and p110β. The boxes include the p85- and Ras-binding domains, the PI3K-C2-, helical- and catalytic domains. Information on domain localisation gathered from UniProtKB ID number P42336 (for p110α) and P42338 (for p110β). A) Domain structure of p110α. B) Domain structure of p110β. Nuclear localisation signal (NLS) motif included in C2 domain of p110β.

2.2 Nuclear PPIn and PI3Ks

The metabolic cycle of PPIn in the cytoplasm was discovered as far back as the 1950s, but another 30 years of research was required before the nuclear pool of PPIn was revealed. Findings by Smith and Wells in 1983 demonstrated that PtdIns and some of their metabolising kinases (class I PI3Ks) were indeed present in the nucleus of rat liver cells (Smith and Wells, 1983). Slowly but surely, it became clear that not only were PPIn present in the nucleus, but they existed independently of the nuclear membrane and the cytosolic PPIn pool (Cocco *et al.*, 1987). Indeed, studies have documented the presence of all PPIn in the nucleus, except for PtdIns(3,5)P_2 (Barlow *et al.*, 2010). Based on the presence of lipids within the nucleus there must be proteins and receptors also localised here that contain hydrophobic domains that can sequester the fatty acyl chains of the PPIn (Blind *et al.*, 2014). This type of interaction is different from the effector proteins that bind the inositol ring of the PPIn, however.

As this thesis has focused on PIP3, the emphasis will be put on this nuclear PPIn for further discussion about localisation, metabolism, and interacting proteins and enzymes. Nuclear mono- and di-phosphorylated PPIn will not be discussed in detail.

2.2.1 Nuclear PIP3 and PI3K pathway

Several studies have demonstrated that members of the PI3K pathway, both kinases and phosphatases, PtdIns(4,5)P_2 and PIP3 are indeed localized in the nucleus and have distinct functions (Lindsay *et al.*, 2006; Davis *et al.*, 2015), as seen in **Table 2.1**. For example, Boronenkov *et al*. found that PtdIns(4,5)P_2, the substrate of p110β, was found clustered around speckles of interchromatin in the nucleus by immunostaining (Boronenkov *et al.*, 1998; Osborne *et al.*, 2001). PIP3 was found in the nuclear matrix (Lindsay *et al.*, 2006) and nucleolus of human breast cancer cells (Karlsson *et al.*, 2016). The pool of nuclear PPIn is regulated by the PI kinases and phosphatases also present in the nucleus, of which class I PI3Ks have been shown to localize (Kumar *et al.*, 2010; Karlsson *et al.*, 2016). The generation of PIP3 in the nucleus is likely governed by the class I PI3K isoform p110β, but also inositol polyphosphate multikinase (IPMK) (Resnick *et al.*, 2005; Kumar *et al.*, 2010). The presence of PI3K in the nucleus in different cells comes from the translocation mediated by the regulatory p85 subunit, which occurs upon different stimuli (earlier studies reviewed in (Neri *et al.*, 2002)). In a previous study, Neri *et al*. demonstrated that nerve growth factor induced the nuclear translocation of p85 in PC12 cells, which also led to increased nuclear p85-dependent PI3K activity and nuclear PIP3 synthesis (Neri *et al.*, 1999). It is also important to note that upon inhibition by a pan-PI3K inhibitor like wortmannin, the production of the nuclear PIP3 pool was blocked (Lindsay *et al.*, 2006), further strengthening the belief that this pool is indeed made by p110β.

Table 2.1. Nuclear PtdIns(4,5)P_2 and PtdIns(3,4,5)P_3, their effector proteins and cellular function. Abbreviations: ALY (THO complex subunit 4), EBP1 (ErbB3-binding protein 1), PIKE (PI3-Kinase Enhancer), SF-1 (steroidogenic factor-1), Topo IIα (DNA Topoisomerase IIα)

PPIn	PPIn nuclear localisation	Reference	Effector proteins	Function of interaction	Reference
PtdIns (4,5)P_2	Nuclear speckles Nucleolus Nuclear islets	(Boronenkov *et al.*, 1998; Osborne *et al.*, 2001; Sobol *et al.*, 2018)	Topo IIα	DNA topology	(Lewis *et al.*, 2011)
			ALY	Cell proliferation	(Okada *et al.*, 2008)
			SF-1	Nuclear receptor Steroidogenesis	(Blind *et al.*, 2012)

PtdIns (3,4,5)P_3	Nuclear matrix Nucleolus	(Lindsay *et al.*, 2006; Kwon *et al.*, 2010; Kumar *et al.*, 2011; Karlsson *et al.*, 2016)	Nucleophosmin /B23	Promote cell survival	(Ahn *et al.*, 2005)
			ALY	Cell proliferation	(Okada *et al.*, 2008)
			PIKE	Cell survival	(Ye *et al.*, 2000)
			Akt ALY	Transcription factor phosphorylation	(Kwon *et al.*, 2010)
			EBP1	Unknown	(Karlsson *et al.*, 2016)

Kumar *et al*. have shown that there exists a nuclear localization signal (NLS) within the C2 domain of p110β, that the isoform concentrates in the nucleus, and that overexpression of the kinase is retained in the cytoplasm (Kumar *et al.*, 2011). In the same study, they found that nuclear, but not cytosolic p110β was essential for cell survival in mouse cells, and that p110β can shuttle in and out of the nucleus to the cytoplasm by way of the regulatory subunit p85β. p110β has been shown to be involved in multiple vital cellular functions such as DNA replication, cell cycle progression and DNA double strand break (DSB) repair (Marques *et al.*, 2008, 2009, Kumar *et al.*, 2010, 2011).

2.2.2 Nuclear PIP3 effector proteins

As mentioned in section **2.1.1**, for PPIn to be effective as signal transducers, they must bind to an effector protein with a PI-domain, like the PH-domain or a KR-motif. Only a few PIP3-binding proteins have been found in the nucleus, however. These include PtdIns(3,4,5)P_3-binding protein (PIP3-BP) found in the brain, PIKE (L-isoform of PI3K enhancer), the mRNA export protein ALY (THO complex subunit 4), and the nucleolar protein nucleophosmin, which has been reported to associate with PIP3 (Tanaka *et al.*, 1999; Ahn *et al.*, 2005; Hu *et al.*, 2005; Wickramasinghe *et al.*, 2013). Also, recently PIP3 was found to interact with Erb-B3-Binding Protein 1 (EBP1) in the nucleolus, where interestingly, the nucleolar localization of EBP1 was lost when the PIP3 binding motif was mutated (Karlsson *et al.*, 2016).

So far, a few nuclear PPIn-interacting proteins have been discovered, studied and characterized individually (Schramp *et al.*, 2012; Shah *et al.*, 2013; Hamann and Blind, 2018). In order to look at nuclear PPIn and their effector proteins, nuclear fractionation was combined with interactomics (Lewis *et al.*, 2011). Using this method, Lewis *et al*. identified PtdIns(4,5)P_2 nuclear interacting proteins involved in mRNA splicing and protein folding. Nuclear PPIn usually regulate their processes by interacting with proteins containing KR-motifs, instead of typical PI-binding domains (Hammond and Balla, 2015). Considering that the key signalling lipid PIP3, together with its kinase p110β, are present in the nucleus and nucleolus, our group performed mass spectrometry based PIP3 interactomics on HeLa nuclei developed by Lewis *et al*. (Lewis *et al.*, 2011). The results identified 219 potential PIP3-binding proteins, involved in several cellular processes, including RNA processing, mRNA splicing and DNA repair (Mazloumi Gavgani *et al.*, 2017). Of these, 29% belonged to the nucleolar database, including PARP1 (Scott *et al.*, 2011).

2.2.3 PARP1

ADP-ribosylation is a post-translational modification (PTM) that typically occurs by the addition of long chains of ADP-ribose, called Poly(ADP-ribosyl)ation, which are linked through glycosidic ribose-ribose bonds (D'Amours *et al.*, 1999). This PTM has been shown to be part of many processes, including mitosis, apoptosis, transcriptional regulation and DNA damage repair (Kim *et al.*, 2005).

Poly(ADP-ribosyl)ation is carried out by a family of proteins called Poly(ADP-ribosyl) polymerase (PARP), which was first reported more than 50 years ago (Chambon *et al.*, 1963). The PARP family contains a highly conserved catalytic domain and other motifs, including two N-terminal zinc-fingers, a double nuclear localisation signal (NLS) and a "BRCA1 C-terminus-like" (BRCT) motif (Amé *et al.*, 2004). In the following years, the founding member of the family, PARP1, was extensively studied. PARP1 functions by synthesizing poly(ADP-ribose) from the donor molecule nicotinamide adenine dinucleotide (NAD^+), and adding it onto a nuclear acceptor protein (Hassa and Hottiger, 2008).

2.3 PIP3 and PI3K in the nucleolus

2.3.1 An introduction to the nucleolus

In eukaryotes, the nucleus is divided into several sub-compartments where specific, nuclear activities take place during interphase. The nucleolus is one such sub-compartment, and is the biggest subnuclear structure (Nemeth and Langst, 2011). Amongst other functions, nucleoli oversee the biogenesis of ribosomes, vital in protein translation. Ribosomes are composed of four specific ribosomal RNAs (rRNAs) and multiple ribosomal proteins. In humans, expression of ribosomal gene loci (18S, 5.8S and 28S) happen on acrocentric chromosomes, namely chromosomes 13, 14, 15, 21 and 22, which are mostly tandem repeats of ribosomal genes. Nucleoli form around these loci, called nucleolar organizer regions (NORs), which are located on the short arms of these acrocentric chromosomes (McStay, 2016).

Transcription of rRNA is carried out by RNA polymerase I (Pol I). During pro-phase, the initiation of mitosis, Pol I transcription is shut down, and nucleoli in many cells disappear (McStay, 2016). In the beginning of telophase, Pol I transcription resumes, and numerous small nucleoli begin to form around individual NORs (Savino *et al.*, 2001). As the cell cycle progresses, nucleolar fusion takes place, resulting in the formation of a few larger, mature nucleoli, which contain multiple NORs (McStay, 2016). Due to their low DNA content, nucleoli are generally seen as dark spots in DAPI- or Hoechst-stained nuclei (McStay, 2016).

In mammalian cells nucleoli are comprised of three distinct sub-compartments that can readily be seen with an electron microscope. These compartments are the innermost fibrillar centre (FC), surrounded by dense fibrillar components (DFC), which are in turn surrounded by granular components (GC) (Pederson, 2011; Farley *et al.*, 2015), see **Figure 2.3**. Ribosome biogenesis is regarded as a vectoral process that initiates in FC and proceeds outward toward the GC, and is one of the most energetically demanding processes in the cell (Thomson *et al.*, 2013). The FC contains the ribosomal genes, and rRNA transcription takes place in the border between FC and DFC. First, the 47S rRNA precursor is transcribed, flanked by 5' and 3' external transcribed spacers (ETS), and undergoes multiple maturation steps to eventually become the 18S, 5.8S and 28S rRNAs. These then assemble with ribosomal proteins to form the 40S and 60S subunits of the ribosome in the GC, together with the 5S subunit, which is transcribed outside the nucleolus by RNA polymerase III. The large and small subunits are then exported to the cytoplasm for final maturation (McStay, 2016).

The nucleolus is surrounded by a heterochromatin shell, which mostly contains silent DNA. Also present is the perinucleolar compartment (PNC), which was first described when the polypyrimidine-tract binding protein was found to localize there (Ghetti *et al.*, 1992). PNC also contains many RNA binding proteins and RNA polymerase III transcripts, like 5S (Pollock and Huang, 2010). Generally speaking, the structure of the nucleolus is considered a direct consequence of ribosome biogenesis, rather than any skeletal framework, and the architecture is dependent on ongoing transcription (Hadjiolov, 1985). This is due to the nucleolar proteins being highly dynamic, able to translocate between the nucleolus and nucleus (Misteli, 2001).

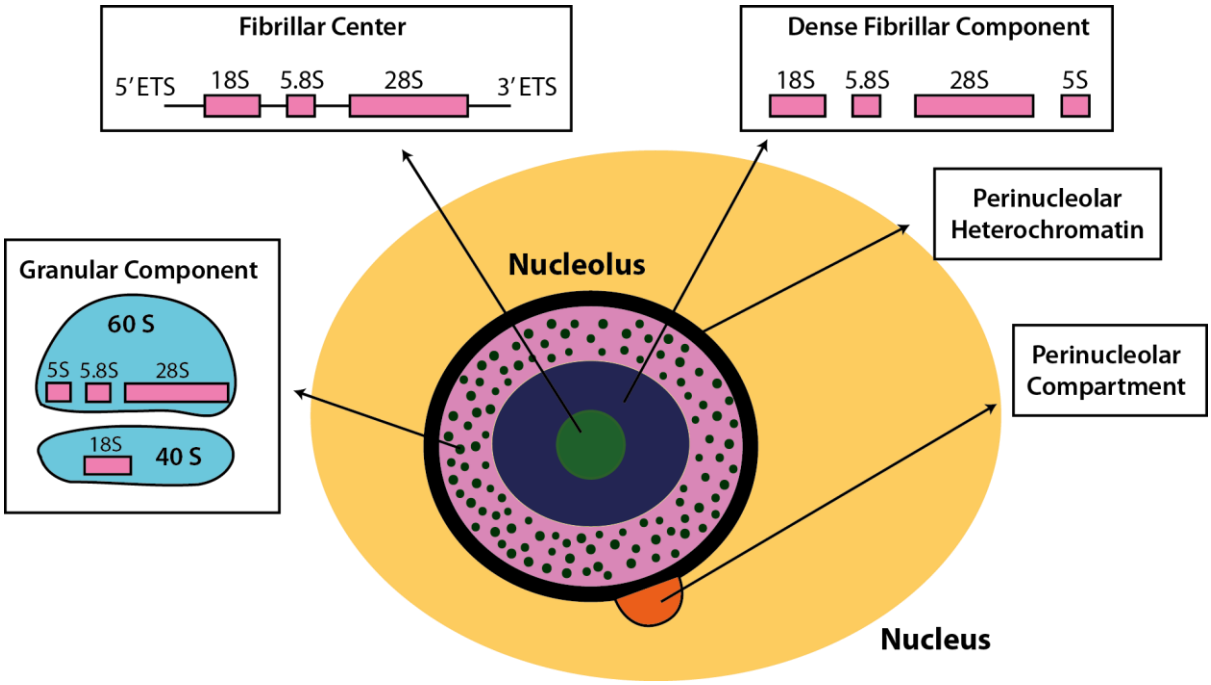

Figure 2.3. Diagram of the compartments in and around the nucleolus. Transcription of rRNA by RNA polymerase I occurs at the boundary between the innermost fibrillar centre (FC) and the dense fibrillar components (DFC). The rRNA is processed to yield the 18S, 5.8S and 28S subunits in the DFC before fusing with the 5S and other ribosomal proteins in the granular components (GC) to assemble the 40S and 60S subunits of the ribosomes. After formation, they are exported from the nucleolus. Around the nucleoli lies a heterochromatin shell mostly containing silent DNA, called perinucleolar heterochromatin. A small structure also associated with the nucleolar surface is the perinucleolar compartment, which contains a lot of RNA binding proteins and RNA polymerase III transcripts. Drawing based on Mazloumi Gavgani (2017).

2.3.2 PI3K and its involvement in rRNA transcription

In recent years PPIn and some of their metabolizing enzymes have been reported in the nucleolus, see **Table 2.2**, and our group has recently mapped p110β and PIP3 in the nucleolus of the human breast cancer cell line AU565 (Karlsson *et al.*, 2016).

Table 2.2. PPIns and PPIn-metabolizing enzymes identified in the nucleolus.

PPIn/PI-enzymes	**Identified functions in the nucleolus**	**References**
PtdIns(4,5)P_2	Promotes Pol I transcription, but not as a source for DAG and IP_3	(Yildirim *et al.*, 2013)
	Structural role	(Sobol *et al.*, 2013)
PtdIns(3,4,5)P_3	Unknown	(Karlsson *et al.*, 2016)
PI4K230/IIIα	Possibly in complex with DNA and RNA	(Kakuk *et al.*, 2006, 2008)
PIP5KIα	Member of rDNA silencing complex	(Chakrabarti *et al.*, 2015)
p110β	Unknown	(Karlsson *et al.*, 2016)
PTEN	Contributes to phenotypic changes of the nucleolus	(Li *et al.*, 2014)
SHIP1	Localises in the nucleolar cavity upon proteasome inhibition, unknown function.	(Ehm *et al.*, 2015)

The PI3K pathway regulates key nucleolar proteins, including the upstream binding transcription factor (UBF) 1 and transcription initiation factor-I (TIF-I) (Nguyen and Mitchell, 2013; Yildirim *et al.*, 2013). Drakas *et al*. demonstrated that insulin receptor substrate 1 (IRS-1), an important docking protein involved in the Pol I promoter complex, can translocate to the nucleolus, where it stimulates phosphorylation of UBF by a PI3K isoform (Drakas *et al.*, 2004). Seeing as p110β is present here, it is likely this isoform that is involved. In 2013, a study showed that Akt was involved in activating and stabilizing TIF-1, also essential in the Pol I promoter. Activation of Akt led to increased rRNA transcription, demonstrating that Akt may be involved in promoting tumour cell proliferation (Nguyen and Mitchell, 2013). Yildirim *et al*. found that the PI3K substrate PtdIns(4,5)P_2 is a part of the RNA transcriptional promoter,

by binding to UBF and the pre-rRNA processing factor fibrillarin, which in turn allows their binding to DNA and RNA respectively (Yildirim *et al.*, 2013).

2.4 The PI3K pathway and its involvement in cancer

The PI3K signalling pathway is involved in continued cell survival, and activating mutations can lead to diseases like cancer. Meanwhile, inactivating mutations can lead to other kinds of diseases, like myopathy and neuropathy (Vanhaesebroeck *et al.*, 2012). The many pathways controlled by the different PI3K isoforms and their downstream signalling are vital in maintaining the balance required for proper cell development, growth and survival.

2.4.1 The PI3K pathway in cancer

The PI3K/Akt/mTOR signalling pathway is one of the most altered pathways in human cancers with frequent mutations in several of its components (Cully *et al.*, 2006; Rozengurt *et al.*, 2014). When regarding the different PI3K isoforms, the most noticeable is the high frequency of activating *PIK3CA* (the gene coding for p110α) mutations in various solid cancers (Samuels *et al.*, 2004). In their study, wherein they sequenced the *PIK3CA* genes from different human cancers, Samuels *et al.* found the mutations occurred later on in tumorigenesis, located on the helical and kinase domains of the gene. Mutations in the other isoforms is uncommon, though activating mutations of the *PIK3CD* gene (coding for p110δ) have been linked to diseases of the respiratory and immune systems (Angulo *et al.*, 2013). Mutations in the *PIK3CB* gene (coding for p110β) have also been reported in a couple of reports (Dbouk *et al.*, 2013; Pazarentzos *et al.*, 2016).

As mentioned, the natural antagonist to the PI3K pathway is the phosphatase and tensin homolog (PTEN), which reverts PIP3 to PtdIns(4,5)P_2. Mutations that lead to loss-of-function of this protein have been linked to multiple human cancers, including glioblastoma, prostate and breast cancer (Li *et al.*, 1997). Interestingly, PTEN-deficient mouse prostate tumours have been shown to be dependent on the lipid kinase activity of the *PIK3CB* gene product, p110β, rather than the alpha isoform (Berenjeno *et al.*, 2012). With more research and a better understanding, it becomes more and more clear that there exists a need to tailor therapeutic approaches based on the specific PI3K isoform, in order to achieve optimal treatment response.

2.4.2 PI3K and endometrial cancer

There is a large variety of human cancers, but one of the most common female gynaecological cancers in the developed world is endometrial cancer (EC), also known as cancer of the corpus

uteri (Ferlay *et al.*, 2015). In Europe and North America, uterine cancers accounted for 6% of new cancer cases, and 3% of cancer deaths in 2015 (Murali et al. 2014; Cancer Research UK). It arises in the inner lining of the uterus, the endometrium, and due to its abnormal symptoms, this cancer is often diagnosed at early stages, with prognosis worsening with later stages. EC is more common in women post-menopause, though it also appears in younger women, and the incidence of this cancer is increasing for all ages (Evans-Metcalf *et al.*, 1998; Wartko *et al.*, 2013), with more than 50% attributable to being overweight or obese (Onstad *et al.*, 2016).

EC was divided into two subgroups, type I and II, by Bokhman in 1983, with type I carcinomas being linked to women with obesity, being oestrogen dependent, accounting for approximately 65% of EC patients, and having high survival rates. Type II EC was observed as less common and high grade, arising in approximately 35% of cases, but appearing in women without the signs stated above, and being oestrogen independent, with a worse prognosis (Bokhman, 1983). This view is slightly outdated and disputed, however, and some claim that EC requires a genomic classification of the carcinomas, so as to better create effective, personalized treatment (Murali *et al.*, 2014). Due to the unique genetic makeup of each cancer, and the heterogeneity of the different molecular subgroups, the risk assessment the patients receive often ends with over or under treatment (Stelloo *et al.*, 2016).

In type I EC tumours, the most common cancer-causing mutations are in the *PTEN*, *PIK3CA* and *KRAS* genes (Kandoth *et al.*, 2013). The rate of mutations in the *PIK3CB* gene is low, when comparing it to mutations in *PIK3CA*. However, in 2016, Pazarentzos *et al*. showed an activating mutation within the kinase domain of p110β in multiple carcinomas, including EC, which lead to increased tumour volume (Pazarentzos *et al.*, 2016). Our group has studied the *PIK3CB* mRNA levels in an extensive cohort of patient tumour samples, showing an increase early in cancer progression, from complex atypical hyperplasia to grade 1 lesions. mRNA levels remain high in grade 2 and 3 lesions as well, in both endometrioid and metastatic lesions (*Karlsson et al*., 2017).

Because of the high frequency of PI3K mutations in EC, multiple inhibitors of this pathway are already in clinical trials, including Pilaralisib, a pan-PI3K inhibitor (Matulonis *et al.*, 2015). With the majority of endometrial carcinomas being endometrioid and diagnosed early, treatment is often surgical, though treatment of advanced disease is more complex. Treatment of these high-risk cases has proven to be difficult with regard to drug- and chemoresistance and

eventual recurrence of the cancer (Moxley and McMeekin, 2010). Since so many EC cases harbour mutations resulting in PTEN deficiency, a recent clinical trial using a p110β-specific inhibitor on PTEN-negative cells showed some advantageous effects on 3 patients with endometrial cancer (Mateo *et al.*, 2017). Another study used small interfering RNA to inhibit p110β in PTEN-negative EC cells, which resulted in increased apoptosis and decreased tumour cell proliferation (An *et al.*, 2007). This is promising, as it shows the potential effects of specifically inhibiting this kinase in PTEN-deficient tumours and rationalizes the need to further study the mechanism of function of p110β.

2.5 Aims

The PI3K pathway is pivotal in many important cellular processes. It regulates and controls multiple signalling paths, consisting of a myriad of proteins and lipids. Much of the pathway is understood, but the complexity increases due to the distinct subcellular localizations of different PI3K isoforms and their lipid products. PIP3 is an important second messenger, and both this lipid and its kinase, p110β, have been placed in the nucleolus in a breast cancer cell line (*Karlsson et al*., 2016). Its role in the nucleolus is still poorly understood, however. In a recent study, our group has shown that p110β protein levels are elevated in EC cell lines and that mRNA levels are increased in grade 1 endometrioid endometrial lesions compared to complex hyperplasias (*Karlsson et al*., 2017). These results combined with the presence of this isoform in the nucleolus suggest a possible nucleolar role of p110β in EC. To try to understand the possible nucleolar role of PIP3, our group performed mass spectrometry based PIP3 interactomics on HeLa nuclei developed by Lewis *et al*.. This study revealed the identification of numerous nucleolar proteins in complex with PIP3, including PARP1. These interesting findings lead us to wonder if PARP1 indeed does bind PIP3 directly.

This thesis aims to shed light on some of the nucleolar properties of p110β and its lipid product PIP3, with regards to rRNA transcription, with the following aims:

1. To validate the subnuclear localization of p110β in endometrial cancer cells.
2. To elucidate if p110β contributes to rRNA transcription.
3. To discover the lipid binding properties of the PIP3 effector protein PARP1.

3 Materials

3.1 Chemicals

Chemical	**Abbrev./ Formula**	**Grade/ Purity**	**Supplier**	**Catalog #**
2-[4-(2-Hydroxyethyl)1-piperazinyl] ethansulfonic acid	HEPES		Merck	1.10110
2-amino-2-hydroxymethyl-1,3-propanediol, Trizma® base	Tris	ANG	Sigma-Aldrich®	T6066
30% Acrylamide/Bisacrylamide			BioRad	161-0158
4-(1,1,3,3,-Tetramethylbutyl)phenyl-polyethylene glycol	Triton® X-100	MBG	Sigma-Aldrich®	T8787
Agarose, SeaKem® LE	Agarose	ELG	Lonza	50004
Ammonium persulfate	APS		BioRad	161-0700
Ampicillin	Amp		Sigma-Aldrich®	A9393
Bovine Serum Albumin	BSA		Sigma-Aldrich®	A7906
Bovine Serum Albumin, essentially fatty acid free	BSA essentially free		Sigma-Aldrich®	A8806
Calcium chloride	$CaCl_2$		Merck	1.02083
Chloroform	$CHCl_3$		Sigma-Aldrich®	32211
Dimethyl Sulfoxide	DMSO		Sigma-Aldrich®	472301
Disodium hydrogen phosphate	$Na_2HPO_4 \cdot 2$		Merck	1.06580
DL-Dithiothreitol	DTT		Sigma-Aldrich®	D9163
Ethanol	EtOH		Kemetyl	600051
Ethidium Bromide	EtBr		Sigma-Aldrich®	E1510
Glycerol, Ultra-pure	Glycerol	≥99.5%	Thermo Fisher Scientific	15514011
Igepal CA-630	Igepal		Sigma-Aldrich®	32213
Imperial protein stain	Coomassie		Thermo Fisher Scientific	2461565
Isopropanol	IPA		Kemetyl	600079

Isopropyl-B-D-thiogalactopyranoside	IPTG		Apollo Scientific	BIMB1008
LB Agar		MBG	Sigma-Aldrich®	L2897
Magnesium Chloride	$MgCl_2$	ANG	Merck	1.05833
Methanol	MeOH		Sigma-Aldrich®	32213
N,N,N',N'-tetramethylethylenediamine	TEMED		BioRad	161-0800
Non-fat milk powder			Sainsbury's	-
Paraformaldehyde	PFA		Merck	K40988605
Peptone from casein (Tryptone)	Tryptone		Merck	1.07213
Phenol-chloroform-isoamyl alcohol mixture			Sigma-Aldrich®	77617
Polyoxyethylenesorbitan monolaurate	Tween®20		Sigma-Aldrich®	P1379
Potassium chloride	KCl	ANG	Merck	1.04936
RNA Grade Glycogen			Thermo Fisher	R0551
Sodium azide	NaN_3		Marck	1.06688
Sodium chloride	NaCl	≥99.5%	Sigma-Aldrich®	31434N
Sodium dihydrogen phosphate	$NaH_2PO_4 \cdot H_2O$		Merck	1.60346
Titriplex® ethylenedinitrilotetraacetic acid disodium salt dehydrate	EDTA	ANG	Merck	1.08418
TRI Reagent®	Trizol		Sigma-Aldrich®	T9424
Yeast extract			Merck	1.03753

MBG- molecular biology grade, CCG- cell culture grade, ELG- electrophoresis grade, ANG- analysis grade.

Table 3.2 Cell culture reagents

Chemical	Supplier	Catalog #
Dulbecco's modified eagles' medium (DMEM) high glucose (containing L-Glu and 4500 mg/L Glucose)	Sigma Aldrich®	D6429
Dulbecco's modified eagles' medium (DMEM) low glucose (containing L-Glu and 1000 mg/L Glucose)	Sigma Aldrich®	D6046
Fetal Bovine Serum (FBS)	Sigma Aldrich®	F7524
100x Penicillin-Streptomycin (PEN/STREP)	Merck	TMS-AB2-C
Trypsin-EDTA	Sigma Aldrich®	T4049

Table 3.3 Commercial kits and reagents

Name	Supplier	Purpose
SuperSignal® West Pico Chemiluminescence	Thermo Fisher Scientific	Western Blot Visualization
SuperSignal® West Femto Maximum Sensitivity Chemiluminescence	Thermo Fisher Scientific	Western Blot Visualization
Nitrocellulose blotting membrane	GE Healthcare Life Science	Western Blot
Kin193 (5 mg)	Selleck Chemicals	p110β inhibition
BMH21 RNA Polymerase I inhibitor	Selleck Chemicals	Pol I inhibition
NucleoSpin® Plasmid	Macherey-Nagel	Miniprep
NucleoSpin® Gel and PCR Clean-up	Macherey-Nagel	Plasmid purification
High-Capacity cDNA Reverse Transcription Kit	Thermo Fisher Scientific	qPCR
LightCycler® 480 SYBR Green I Master	Life Science / Roche	qPCR
PowerUp™ SYBR™ Green Master Mix	Thermo Fisher Scientific	qPCR
Click-iT™ RNA Alexa Fluor™ Imaging Kit	Thermo Fisher Scientific	RNA visualisation
PIP Strip Lot # XCM100316-48	Echelon	Lipid overlay assay
InstantBlue	Expedeon	Coomassie staining
BigDye v 3.1	Thermo Fisher Scientific	Sequencing
Sequencing buffer	Thermo Fisher Scientific	Sequencing
ProLong® Gold antifade reagent with Hoechst	Thermo Fisher Scientific	Cover slip mounting
Goat serum	Thermo Fisher Scientific	Blocking

Table 3.4 Bacteria

Name	Supplier	Purpose
Escherichia coli Subcloning Efficiency™ DH5α™ competent cells	Thermo Fisher Scientific	Plasmid purification
Escherichia coli BL-21 CodonPlus® (DE3)-RIL Competent Cells	Agilent	Protein expression

Table 3.5 Cell lines

Name	Description	Supplier
RL95-2	Human endometrial carcinoma	Prof. Helga B Salvesen, University of Bergen
MEF p110β WT	p110β wild type mouse embryonic fibroblast	Dr Julie Guillermet-Guibert, University of Toulouse, France
MEF p110β KI (D931A/D931A)	Kinase inactive for p110β mouse embryonic fibroblast	Dr Julie Guillermet-Guibert, University of Toulouse, France

Table 3.6 Antibodies

Name	Supplier	Catalog #	Species	Dilution
p110β	Cell Signalling	C33D4	Rabbit	1:50 IMF 1:2000 WB
p110β	Abcam	Ab151549	Rabbit	1:50 IMF 1:2000 WB
PIP3	Echelon	ZP345b	Mouse	1:400 IMF
Nucleolin	Cell Signalling	D4C70	Rabbit	1:100 IMF
Nucleophosmin	Thermo Fisher Scientific	FC-61991	Mouse	1:1000 IMF
Fibrillarin	Cell Signalling	C13C3	Rabbit	1:5000 WB
α-Tubulin	Sigma Aldrich®	T5168	Mouse	1:10000 WB
Lamin A/C (E1)	Santa Cruz	sc-376248	Mouse	1:10000 WB
Goat anti-rabbit IgG (H+L), horseradish peroxidase conjugate	Life Technologies	G21234	Rabbit	1:5000 WB
Goat α-rabbit IgG1 (γ1); Alexa Fluor® 488-conjugated	Thermo Fisher Scientific	A11008	Rabbit	1:200 IMF
Goat α-mouse IgG (H+L); Alexa Fluor® 594-conjugated	Thermo Fisher Scientific	A11005	Mouse	1:200 IMF

IMF – Immunofluorescent staining, WB – Western blotting.

Table 3.7 Equipment

Name	Supplier	Software	Purpose
ChemiDoc XRS+™	BioRad	ImageLab	WB imaging
GelDoc EZ Imager	BioRad	ImageLab	Agarose and SDS-PAG imaging

Epoch microplate Spectrophotometer	BioTek	Gen5	DNA, RNA and protein concentration
Allegra® X-15R Centrifuge	Beckman Coulter		Centrifugation
Avanti® J-26 XP	Beckman Coulter		Centrifugation
Fluorescence microscope DMI 6000 B	Leica Microsystems	Leica Application suite (LAS) X	Fluorescent imaging
Confocal microscope SP5 AOBS	Leica Microsystems	Leica Application suite (LAS) X	Fluorescent imaging

Table 3.8 qPCR primers

Name	Sequence
Human ETS1 Forward	5'-GTGCGTGTCAGGCGTTCT-3'
Human ETS1 Reverse	5'-GGGAGAGGAGCAGACGAG-3'
Human β-Actin Forward	5'-TGCGTCTGGACCTGGCTGGC-3'
Human β-Actin Reverse	5'-GCCTCAGGGCAGCGGAACC-3'
Mouse B2M Forward	5'-CTGCTACGTAACACAGTTCCACCC-3'
Mouse B2M Reverse	5'-CATGATGCTTGATCACATGTCTCG-3'
Mouse ETS Forward	5'-TTTTGGGGAGGTGGAGAGTC-3'
Mouse ETS Reverse	5'-AGAGAACTCCGGAGCACCAC-3'

Table 3.9 Plasmids

Plasmids were obtained from Prof. Michael O. Hottiger, University of Zurich, Switzerland (Hassa *et al.*, 2005), cloned in pGEX-6P-2 into BamHI and NotI.

Fragment #	Name	Amino acids	Size (kDa)
1	PARP1 fragment 1	1-214	24
2	PARP1 fragment 2	215-371	17.7
3	PARP1 fragment 3	477-524	5.1
4	PARP1 fragment 4	525-656	15
5	PARP1 fragment 5	657-1014	40

3.10 Prepared buffers and solutions

Nucleolar fractionation

Buffer A

10 mM hepes pH 7.9
10 mM KCl

1.5 mM $MgCl_2$
0.5 mM DTT
1x Protease inhibitor cocktail*
1% Igepal

Buffer S1
0.25 M sucrose
10 mM $MgCl_2$
1x Protease inhibitor cocktail*

Buffer S2
0.35 mM sucrose
0.5 mM $MgCl_2$
1x Protease inhibitor cocktail*

Buffer S3
0.88 mM sucrose
0.5 mM $MgCl_2$
1x Protease inhibitor cocktail*

* 1 Complete EDTA-free Protease inhibitor cocktail tablet from Roche dissolved in 1 mL H_2O, makes a 50x solution

SDS-PAGE and Western Blotting

Resolving gel
8-12% of 30% acrylamide/ bisacrylamide (37.5:1)
375 mM Tris-HCl pH 8.8
0.1% (v/v) SDS
0.1% (v/v) APS
0.04% TEMED

Stacking gel
5% of 30% acrylamide/bisacrylamide (37.5:1)
125 mM Tris-HCl pH 6.8
0.1% (v/v) SDS
0.1% (v/v) APS
0.04% TEMED

5x SDS Sample Buffer
65 mM Tris-HCl pH 6.8
5% SDS (v/v)
20% glycerol (v/v)
250 mM DTT
0.2% Bromophenol Blue (w/v)

1x Running buffer (TGS)
25 mM Tris pH 8.3
192 mM Glycine
0.1 % (w/v) SDS

1x PBS-T pH 7.4
137 mM NaCl
2.68 mM KCl
8 mM $NaH_2PO_4 \cdot H_2O$
0.05% (v/v) Tween 20

Blocking buffer WB
7% (w/v) powdered skim milk in 1x PBS-T

1x Transfer buffer (TG)
25 mM Tris pH 8.3
192 mM Glycine
20% (v/v) MeOH

Agarose gel electrophoresis

1x TAE Buffer
40 mM Tris base
1 mM EDTA pH 8.0
20 mM Acetic acid

6x DNA Sample Buffer
30% Glycerol
0.025% Bromophenol Blue

Bacterial cultivation

LB medium

1% (w/v) tryptone
0.5% (w/v) yeast extract
1% (w/v) NaCl

LB agar

1.5% (w/v) agar in LB medium

4 Methods

4.1 Cell culture

4.1.1 Cultivation

Cell lines were grown and cultivated in complete media composed of Dulbecco's modified eagles' medium (DMEM), 10% FBS and 1% PEN/STREP. The cells were cultured in 10 or 15 cm round cell culture grade dishes, incubated at 37°C with 5% CO_2. All cell work was performed in a flow bench.

4.1.2 Passaging

To passage cells, media was removed, and the cells were washed once with 1x PBS pH 7.4. PBS was removed, and 0.25% Trypsin was added (0.5 mL for 5 cm plates, 1 ml for 10 cm plates and 2 mL for 15 cm plates) and incubated at room temperature (RT) until cells appeared to condense, but not detach from the plate, which was confirmed by checking under a microscope. The trypsin was removed, and fresh, complete media was added to the dish, and cells were aliquoted in dilutions (1:2, 1:4 or 1:10) to fresh plates, according to need.

When seeding a specific number of cells, cells were trypsinized, medium was added to stop trypsinization, and cells were collected in a 15 mL tube. Cells were centrifuged at 90 x g for 5 min and resuspended in fresh medium. 10 µl of the suspension was loaded onto a slide and inserted into the TC20 automated cell counter from BioRad. The number of cells required was calculated, and cell suspensions were transferred to new plates with fresh medium.

4.1.3 Freezing

Cells were generally frozen at lower passage numbers to maintain a frozen stock cell line. Media was removed from the plate, and the cells were washed once with 1x PBS, before adding 0.25% Trypsin. Cells were allowed to completely trypsinize, before addition of 2-4 mL fresh medium, and collecting into a tube. The cells were centrifuged at 90 x g for 5 min, before resuspending in fresh medium containing 10% FBS and 5% DMSO. The mixture was

transferred to a CryoPure tube and stored at -20°C for 1-2 h before being placed at -80°C for up to 1 month before transfer to liquid nitrogen.

4.1.4 Thawing

After retrieval from liquid nitrogen or the -80°C freezer, cells could gently come up to room temperature, before being spun down at 90 x g for 5 min, to remove DMSO remnants. The pellet was resuspended in 1 mL fresh complete medium, and transferred to a new plate, and allowed to grow at 37°C and 5% CO_2.

4.1.5 Cell treatment

For various treatments performed, initial seeding was the same for both RL95-2 and MEF WT/KI cell lines. Cells were seeded onto 35 mm plates with DMEM (200 000 cells for MEF WT/KI, and 500 000 cells for RL95-2) containing cover slips and grown at cell culture conditions for 24 hours prior to treatment. For serum-free treatment, cells were washed with – and incubated in – serum-free (SF), low-glucose medium for 24 hours. The next day, 20% FBS was added to plates at 37°C with 5% CO_2 for 30 or 60 min, see **Figure 4.1**.

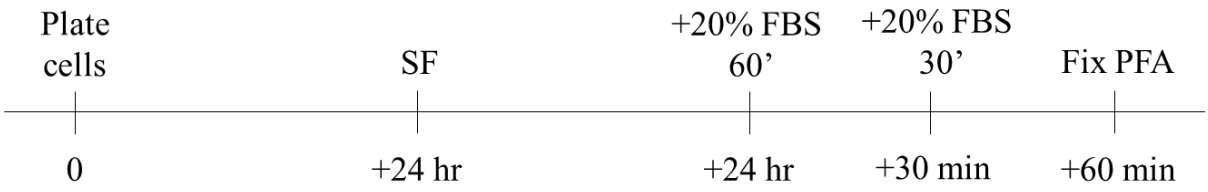

Figure 4.1. Timeline for starvation experiments. Cells were seeded and incubated for 24 hours before changing to serum-free (SF) medium, and incubating a further 24 hours. Cells were then given a boost of 20% foetal bovine serum (FBS) for 60 or 30 min, followed by washing with PBS and fixing with 3.7 or 4% PFA for 10 min. For EU treatment, EU was added to cells 30 min before washing with PBS and fixing.

For specific p110β inhibition with Kin193, 10 µM working solution of Kin193 was used. Cells were grown with high glucose DMEM in cell culture conditions. For the 42-hour treatment, medium was not changed, and instead the cells were washed with PBS and collected for RNA isolation. For 72-hour treatment, medium was changed once, after 42 hours, with new Kin193 added, and grown until the 72-hour mark, then washed and collected. For Kin193 treatment of RL95-2 cells with EU labelling, 10 µM working solution of Kin193 was added to the plates 45 minutes before re-stimulating with serum.

4.2 Immunofluorescent staining and imaging

Cells were grown to 70% confluency and seeded onto coverslips 24 h before staining. Media was removed, and slips were washed once with 1x PBS. The cells were fixed with 3.7% PFA for 10 min at RT and washed three times with PBS, before permeabilization with 0.25% Triton for 15 min at RT. This was followed by blocking non-specific epitopes with blocking buffer containing 5% goat serum and 0.05% Triton in PBS for 1 h at RT, and subsequent addition of primary antibody diluted in blocking buffer (for a list of antibodies used, see section **3.9 Antibodies**). The primary antibody was typically left overnight at 4°C, before washing four times with PBS-T (0.05% Tween 20 in PBS), each wash lasting 5 min at RT. After the last wash, secondary antibody was added, diluted in PBS-T, and incubated at RT for 1 h before washing four times in PBS-T, 5 min each. For double staining, the second primary antibody, raised in a different species, was diluted in blocking buffer and added after the last wash, and incubated at RT for 1-2 h, before washing with PBS-T as described above. The corresponding secondary antibody was added and incubated at RT for 1 h before washing three times with PBS-T, followed by washing once with 1x PBS. The DNA dye Hoechst solution (diluted 1:1000 in PBS) was added to the coverslips for 15 minutes at RT. The slips were then washed twice with PBS and dipped in ddH_2O and mounted cell-side down onto glass slides on 5 µl Gold AntiFade solution and kept in the dark until imaging.

Epifluorescent imaging was done using the Fluorescence microscope DMI 6000 B from Leica Microsystems. More detailed images for studying different cell slices were taken using the confocal microscope SP5 AOBS, also from Leica Microsystems. Images from both microscopes were processed using the Leica Application Suite X software. When images were taken to compare different conditions, treatments or cell lines, acquirement settings (exposure time, intensity and gain) were the same for all slips.

4.3 Nucleolar isolation

Nucleolar isolation from endometrial cancer cells was adapted from Lam *et al.* (Lam and Lamond, 2006). In brief, RL95-2 cells were grown in 10 x 15 cm dishes until 70% confluent, at which point fresh media was added 1 h before harvesting the cells. Plates were trypsinized completely and collected, spun down at 90 x g for 5 min and resuspended in 7 mL complete medium, and spun down again at 230 xg for 5 min. Cells were then washed three times with ice-cold PBS, and centrifuged at 70 x g for 5 min after each wash. The cell pellet was

resuspended in 5 mL of buffer A (**Table 3.2.1**) and incubated on ice for 5 min before they were passed through a 23-gauge needle 16 times on ice to disrupt the plasma membrane, and centrifuged at 70 x g for 5 min. The supernatant was collected as the cytoplasmic fraction, and the nuclear pellet was resuspended in 3 mL buffer S1 (**Table 3.2.1**), which was carefully layered over with 3 mL of buffer S2 (**Table 3.2.1**), and spun down at 1430 x g for 5 min at 4°C. The resulting pellet was resuspended in 3 mL buffer S2 and nuclei were sonicated 7 times 10 sec on/ 10 sec off on ice using the Ultrasonic Homogenizer 4710 from Parmer. The sonicated pellet was carefully layed over 3 mL buffer S3 (**Table 3.2.1**), and spun down at 3000 x g for 10 min at 4°C. The top 3 mL was collected as nucleoplasmic fraction, and the pellet was resuspended in 500 µl of buffer S2, then centrifuged at 1430 x g for 5 min at 4°C. To this, buffer S2 or RIPA buffer was added. All fractions were kept at -80°C.

4.4 EU labelling

To detect nascent RNA, cells were labelled with 5-ethynyl uridine (EU) and visualized by immunofluorescent imaging. Labelling cells with EU was done according to the Click-iT® RNA Imaging Kit from Thermo Fisher Scientific, with 1 mM working concentration of EU. A 2x working solution of EU was prepared from the 100 mM stock in DMEM supplemented with PenStrep and FBS, or in serum-free (SF) medium. The solution was added to the cells so that the final concentration of EU was 1 mM. Treatment lasted for 30 min, and was done together with reboosting with 20% FBS, before washing with 1x PBS and fixing with 4% PFA for 10 min at RT. For immunostaining, slips were permeabilized and blocked as described above. Next, the Click-it reaction cocktail was made as described in the protocol using the Alexa Fluor 594 azide, 500 µl of which was added to each well containing a slip. The reaction was completed in 30 min at RT, and slips were washed with 1 mL of RNA imaging kit reaction rinse buffer. For additional immunostaining, primary antibody was added and left overnight. The following day, secondary antibody and DNA staining was done, and imaging was performed as described, using the Leica confocal microscope SP5 AOBS.

4.5 RNA extraction

Harvesting cells for RNA isolation was generally done in 1x 15 cm plate of 80% confluent cells. When different culture plates were used, volumes were adjusted proportionally. Media was removed, and cells were washed once with PBS before completely trypsinizing and collecting into a tube. This was followed by centrifuging at 70 x g for 5 min and kept on ice.

Media was removed, and pellet was carefully washed with 5 mL PBS and centrifuged at 300 x g for 5 min at 4°C. The cell pellet was resuspended in 1 mL of PBS and centrifuged at 300 x g for 5 min at 4°C. PBS was discarded and the previous centrifugation step was repeated, but for 1 min to remove excess PBS. The pellet was carefully resuspended in 1 mL TRI reagent and incubated at RT for 5-10 min, and frozen at -80°C until needed.

For RNA isolation, all steps were performed at RT, unless otherwise specified. Cells resuspended in TRI reagent were thawed, to which 200 µl chloroform was added. The contents were vortexed for 1 min, then again for 30 sec, before being incubated for 1 min and centrifuged at 12 000 x g for 15 min at 4°C. The top layer was transferred and placed on ice, to which 500 µl phenol chloroform isoamyl alcohol mixture was added on ice. Contents were vortexed for 1 min and incubated for 2 min, then centrifuged at 12 000 x g for 10 min at 4°C. Again, the top layer was transferred on ice, and 500 µl chloroform was added, vortexed for 1 min and incubated for 1 min, then centrifuged at 12 000 x g for 10 min at 4°C. Top phase was collected on ice, and 20 µg of RNA grade glycogen was added along with 500 µl isopropanol, before vortexing for 10 sec and incubating for 20-30 min. After incubation, the solution was centrifuged at 13 000 x g for 20 min at 4°C, and supernatant was discarded. Pellet was resuspended in 1 mL ice-cold 70% ethanol, vortexed for 30 sec, and centrifuged at 8000 x g for 5 min at 4°C. Supernatant was discarded, and pellet was spun down at 8000 x g for 5 min at 4°C to remove any ethanol. RNase free water was added to the pellet (volume depending on pellet size) and vortexed for 5 seconds every 5 min for 20 min. RNA concentration was measured in an Epoch microplate Spectrophotometer, and total RNA was stored in -80°C until needed.

4.6 cDNA synthesis and RT-qPCR

4.6.1 cDNA synthesis

1 µg of total RNA was used to produce 50 ng/µl cDNA with random primers according to the protocol given in the High-Capacity cDNA Reverse Transcription Kit. Transcribed cDNA was stored at -20°C until real-time quantitative PCR (RT-qPCR) was run.

4.6.2 RT-qPCR

RT-qPCR is a technique similar to a regular PCR method, in that it amplifies genes of interest, but in real-time. For the experiments performed in this thesis, the SYBR green fluorescent dye master mix was used, which fluoresces when bound to double stranded (ds) DNA. When the

amount of dsDNA increases, so does the fluorescence. RT-qPCR was performed on a Roche Light Cycler 480 using PowerUp SYBR Green Master Mix from either Life Sciences or Thermo Fisher Scientific to compare 5' ETS transcription in different cell lines under different conditions. cDNA was diluted 1:200 in RNase free water, to a final concentration of 1 ng/µl. cDNA from control cells was used to make standards with concentrations of: 10.0, 2.0, 0.4, 0.08 and 0.016 ng/µl. These were prepared by making a dilution series from cDNA with RNase free water. 1 µl of cDNA from samples and standard was pipetted into a clean 96-well plate in triplicates, one triplicate for the target gene, and one for a suitable reference gene. The plate was kept on ice for the entirety of the setup. Next, a master mix was made for the target and reference genes with forward and reverse primer pairs, as seen in **Table 3.11**, for human or murine 5' ETS as target and human β-Actin or mouse B2M as reference. Master mix also contained LightCycler® 480 SYBR Green I Master and RNase free water, according to the protocol for LightCycler® 480 SYBR Green I Master from Roche or Thermo Fisher Scientific. 19 µl master mix was added to each well containing cDNA, the plate was covered in a clean film and centrifuged at 2000 rpm for 2 min at 4°C.

The PCR program was set up as described in the LightCycler® 480 SYBR Green I Master from Roche or PowerUp™ SYBR™ Green Master Mix from Thermo Fisher Scientific protocol, with annealing temperature set at 58°C for all experiments, with the thermal program as stated below:

Table 3.10. Thermal program for qPCR for LightCycler® 480 SYBR Green I Master from Roche. The amplification program was performed in 42 cycles.

	Temperature (°C)	**Hold**	**Ramp rate (°C/s)**
Pre-incubation	95	5 min	4.4
Amplification	95	10 sec	4.4
	58	15 sec	2.2
	72	30 sec	4.4
Melting Curve	95	5 sec	4.4
	65	1 min	2.2
	97	Continuous	-
Cooling	40	10 sec	1.5

Table 3.11 Thermal program for PowerUp™ SYBR™ Green Master Mix from Thermo Fisher Scientific. The amplification program was performed in 42 cycles.

	Temperature (°C)	**Hold**	**Ramp rate (°C/s)**
Pre-incubation	50	2 min	4.4
	95	2 min	4.4
Amplification	95	15 sec	4.4
	58	15 sec	2.2
	72	1 min	4.4
Melting Curve	95	15 sec	1.6
	60	1 min	1.6
	97	Continuous	0.11
Cooling	40	10 sec	1.5

4.7 Determination of protein concentration

4.7.1 Bicinchoninic acid (BCA) protein assay

To determine the concentration of purified proteins from RL95-2 fractionation, BCA protein assays were performed, and samples were compared to a linear BCA standard curve. 2 µl of sample was pipetted into a 96-well plate in triplicates, along with triplicates of BSA standards ranging in concentration from 0.31-5 mg/mL, increasing two-fold for each concentration. For standards, BSA was diluted in the same buffer the protein sample was kept in. A working solution was prepared using a ratio of 20:1 BCA solution A: BCA solution B. 200 µl working solution was added to each of the used wells in the plate and incubated for 10 min at 37 °C. Absorbance was read at 600 nm using the Epoch microplate Spectrophotometer.

4.7.2 Bradford protein assay

For purified protein samples kept in a DTT-containing buffer, the Bradford method was used to determine their protein concentration relative to a BSA standard curve. 2 µl of each sample was pipetted into a 96-well plate in triplicate, as well as triplicates of BSA standards ranging in concentration from 0.31-5 mg/mL, increasing two-fold for each concentration. For standards, BSA was diluted in the same buffer the protein sample was kept in. Bradford reagent was diluted 1:4 in distilled Milli-Q™ water, and 200 µl was added to each used well. The plate

was incubated at RT for 5-10 min before reading absorbance at 595 nm in an Epoch microplate Spectrophotometer.

For both types of protein concentration assay, a linear standard curve was made in Excel from a scatterplot and used to determine the protein concentration of each sample. The X-axis showed the protein concentration, and the Y-axis showed absorbance at 600/595 nm.

4.8 GST-PARP1 expression and purification

4.8.1 Transformation of competent cells

DH5α

The five PARP1 constructs were supplied by Prof. MO Hottiger (university of Zurich) on filter paper, see Table 3.12, and the DNA was extracted in ddH_2O, before being transformed into Subcloning Efficiency DH5α™ Competent Cells. Cells were thawed on ice in 12 µl aliquots, into which 1 µl DNA was added and the contents was gently mixed by tapping the tube. The cells were incubated on ice for 30 min followed by heat shock treatment at 42°C for 45 sec, before immediately incubating on ice for 2 min. Next, 70 µl prewarmed (37°C) SOC medium was added, and the cells were incubated at 37°C for 1 h. After recovering, the cells were plated on LB agar plates containing ampicillin (100 µg/mL), and grown overnight at 37°C. The following morning, clones were picked and inoculated in 5 mL LB medium containing 50 µg/mL ampicillin overnight at 37°C with 250 rpm shaking. After growing, the plasmids were purified using the NucleoSpin® Plasmid mini-prep kit. The DNA concentration was measured, and purified DNA was stored at -20°C.

BL-21 DE3

To express the desired GST-PARP1 fusion proteins, the purified plasmids were transformed into BL-21 Codon Plus® (DE3)-RIL competent cells from Agilent Technologies. Cells were thawed on ice in 5 µl aliquots, to which 0.5 µl plasmid DNA (above 100 ng/µl) was added and incubated on ice for 30 min. The rest of the transformation was performed as described above, until the plating step. The next day colonies were picked for either small or big scale protein expression.

4.8.2 Small scale protein expression

To check that the fusion proteins could be expressed sufficiently well before being set up for big scale protein expression, one construct was tested to see if cells could reliably express GST-

PARP1. First, 4 colonies were picked from the BL-21 plate and inoculated in 2 mL LB medium containing ampicillin (50 µg/mL) and grown overnight at 250 rpm at 37°C. 200 µl pre-culture was removed and added to 1.8 mL LB with amp (50 µg/mL) and incubated for 3 h at 37°C at 250 rpm. After 3 h, 100 µl bacterial culture was transferred and spun down by pulsing for 10 sec, then adding 40 µl water and 10 µl SDS sample buffer (5X) and boiling at 95°C for 5 min. Remaining culture was induced with IPTG (0.5 mM) and incubated for 3 h at 250 rpm at 37°C, after which cells were collected and prepared for SDS-PAGE as described with un-induced sample. 40 µl un-induced and 20 µl induced bacteria were run on an SDS-PAGE to check protein expression.

4.8.3 Big scale protein expression

The morning after BL-21 transformation and plating, one colony per construct was picked and inoculated in 50 mL LB medium with 50 µg/mL ampicillin overnight at 37°C with 250 rpm. From the remaining pre-culture, 2 mL was transferred into 100 mL LB medium containing 50 µg/mL ampicillin and grown for around 2 h at 37°C with 250 rpm, until the optical density (OD) reached 0.6-0.7 (up to 1). After the desired OD was reached, 1 mL culture was removed, pelleted and stored for SDS-PAGE. The remaining cultures were induced with 50 mM IPTG for 3 h, before OD was read again. 1 mL was taken from the induced culture, pelleted and stored, and remaining cells were harvested by centrifuging at 6000 rpm for 10 min at 4°C. Bacteria were lysed on ice in 5 mL of 25 mM tris pH 8.0, 500 mM NaCl, 0.5% IgePal and 1x bacterial protease inhibitor cocktail. Subsequently, bacteria were sonicated 3 x 30 sec on/30 sec off, and centrifuged at 13000 x g for 15 min at 4°C. 50 µl supernatant and one pellet was kept for SDS-PAGE, the remaining supernatant was pooled and stored at -80°C.

4.8.4 Soluble protein purification:

Supernatants were thawed on ice, to which 600 µl of 50% slurry glutathione-sepharose was added and left overnight, rotating at 4°C. The following day, beads were washed 4 times with 10 ml ice cold PBS, centrifuged at 3000 rpm for 5 min at 4°C between each wash. They were then washed once with 10 ml 50 mM Tris pH 8.0, 100 mM NaCl, and centrifuged at 3000 rpm for 5 min at 4°C. After the last wash, protein was eluted through 4 successive steps with 200 ul of 50 mM Tris pH 8.0, 100 mM NaCl, 0.5 mM DTT with 0.03 g/10 ml reduced glutathione made fresh. Each elution was performed with gentle agitation for 30 min at RT, after which OD was read at 280 nm. Eluates with highest OD were pooled and a Bradford protein assay

was performed to check concentration. SDS-PAGE was performed with samples from un-induced, induced, supernatant, pellet and eluted protein. Purified protein was stored at -80°C.

4.10 Lipid overlay assay

Lipid blots were performed using PIP strips from Echelon (Lot # XCM100316-48), spotted with Lysophosphatidic acid (LPA), Lysophosphocholine (LPC), Sphingosine 1-Phosphate (S1P), PtdIns, PtdIns(3)*P*, PtdIns(4)*P*, PtdIns(5)*P*, Phosphatidylethanolamine (PE), Phosphatidylcholine (PC), Phosphatidic acid (PA), Phosphatidylserine (PS) PtdIns(3,4)P_2, PtdIns(3,5)P_2, PtdIns(4,5)P_2, and PtdIns(3,4,5)P_3. This was used to test which fragments of PARP1 bind directly to lipids. Membranes were blocked protected from light for 1 h at RT on a shaker with 6 mL TBS-T (TBS with 0.1% v/v Tween 20) containing 3% essentially fatty acid free BSA made fresh. To this, 0.5 µg/mL protein was added directly to the membranes and incubated at RT on a shaker for 1 h. Next, the membranes were washed 6 times with TBS-T, 5 minutes per wash, on a shaker at RT. Following washes, anti-GST conjugated to horse-radish peroxidase (HRP) diluted in TBS-T was added and incubated on a shaker at RT for 1 h before being washed as described above (6x 5 min). After the final wash, visualization was done by chemiluminescence using pico or femto kits (See **Table 3.5**) by incubating the membranes at RT for 5 or 1 min at RT respectively, and imaging them using the BioRad ChemiDoc™ XRS+.

4.11 Agarose gel electrophoresis

Agarose gel electrophoresis was used to separate DNA fragments based on size. This is accomplished by subjecting the DNA samples to an electric field, with the negatively charged DNA traveling toward the positive electrode by passing through a porous agarose gel. Gels were made with 1% agarose in 1x TAE buffer, by boiling in a microwave. Once the mixture cooled, Ethidium bromide was added to a final concentration of 0.5 µg/mL and mixed. The agarose solution was poured into a tray with a comb and allowed to solidify. The electrophoresis was started at 70 V and increased to 100 V until the dye front reached about ¾ the length of the gel. Agarose gels were visualized using the BioRad GelDoc™ EZ Imager.

4.12 SDS-PAGE

For the separation of proteins based on molecular weight, sodium dodecyl sulphate polyacrylamide gel electrophoresis (SDS-PAGE) was performed. The protein in the sample was denatured and given a negative charge. By applying an electric field, the proteins will migrate toward the positive electrode at different speeds, according to their molecular weight.

SDS gels were made with 10% acrylamide/bisacrylamide (37.5:1) in 0.75 or 1.5 mm thickness, depending on the amount of sample to be loaded. Protein samples were mixed with 5x SDS sample buffer to a final concentration of 1x. Samples were boiled at 100°C for 5 min, spun down and kept on ice until loading onto the gel. Electrophoresis was performed in 1x TGS buffer. Samples were run through the stacking gel at 70 V, and 170 V through the resolving gel, until the dye front left the gel. The gel was either used for staining and imaging with Coomassie, or proteins were transferred to a membrane for western immunoblotting.

4.13 Coomassie staining

For visualizing proteins from SDS-PAGE, gels were incubated in about 20 mL InstantBlue (a Coomassie based stain) for 1 h at RT on a shaker. After an hour, the staining solution was replaced with distilled Milli-Q™ water (ddH_2O) for 1-2 h on a shaker, before photographing in the BioRad GelDoc™ EZ Imager.

4.14 Western immunoblotting

Proteins were transferred from SDS gels to a nitrocellulose membrane at 16 V overnight on a shaker in 1x TG buffer. After transfer, the membrane was washed several times in 1x PBS-T (0.05% Tween20) and blocked with 7% powdered fat-free milk dissolved in PBS-T for 1 h on a shaker. This was followed by rinsing once with PBS-T, before adding primary antibody and leaving overnight at 4°C on a shaker. The next day, blots were washed three times in PBS-T, then incubated with secondary antibody (α-mouse/rabbit-HRP 1:10000) for 1 h at room temp on a shaker, kept dark. Secondary antibody was washed off, and blots were rinsed 4 times in PBS-T. For visualization, blots were treated with ECL (pico/femto) for 5 or 1 min, depending on the kit, and photographed in a BioRad ChemiDoc™ XRS+ and stored in PBS-T at 4°C.

5 Results

5.1 p110β is located within the nucleoli of RL95-2 cells

Previously, our group has determined that *PIK3CB* mRNA levels are elevated in endometrial tumours, and that levels increase from precursors to low grade primary lesions (*Karlsson et al.*, 2017). In addition, the protein levels were elevated in a panel of endometrial cancer cell lines compared to non-transformed cells. However, how elevated levels of p110β contribute to tumour development remain unclear. p110β has previously been found to localise in the nucleus in NIH 3T3 cells (a murine cell line) (Kumar *et al.*, 2011), and in nucleoli of human breast cancer cells AU565 (Karlsson *et al.*, 2016). The focus of this thesis was to establish the localization of p110β in a single EC cell line with high levels of p110β. The PTEN-negative human EC cell line RL95-2 was chosen. Our group has preliminary data demonstrating that these cells contain a high PIP3 pool and high levels of p110β in the nucleus, and increased pre-rRNA transcription levels (Mazloumi Gavgani *et al.*, 2017), making this an appropriate cell line to study.

Immunofluorescence staining was performed to establish co-localisation between p110β and a known nucleolar protein, in this case nucleophosmin (NPM). NPM is a protein involved in rRNA transcription (Murano *et al.*, 2008). Consistently, p110β was shown to co-localise with nucleophosmin in the nucleolus, as seen in **Figure 5.1 A**. p110β could also clearly be seen in the cytoplasm in most of the cells, with a weaker signal intensity in the nucleoplasm.

In addition, to validate the results shown by immunofluorescence staining, RL95-2 cells were fractionated, and equal amounts of protein from cytoplasmic, nucleoplasmic and nucleolar fractions were resolved by SDS-PAGE. Western blotting with anti-p110β antibody revealed that p110β was present within the nucleolar compartment of these cells, as well as in the cytoplasm and nucleoplasm, see **Figure 5.1 B**. The purity of each fraction was verified using antibodies against proteins that should be present in each fraction. α-tubulin, a protein of the cytoplasmic cytoskeleton, showed a clear band in the cytoplasmic fraction, and was missing from the other two. Fibrillarin, which is associated with maturation of rRNA in the nucleolus, is found solely in the nucleolar fraction. Lamin A/C, which is typically localized at the nuclear periphery, is also a component of the nuclear matrix (Gruenbaum and Foisner, 2015), and was thus present throughout the nucleus, including the nucleolus, and absent from the cytoplasm.

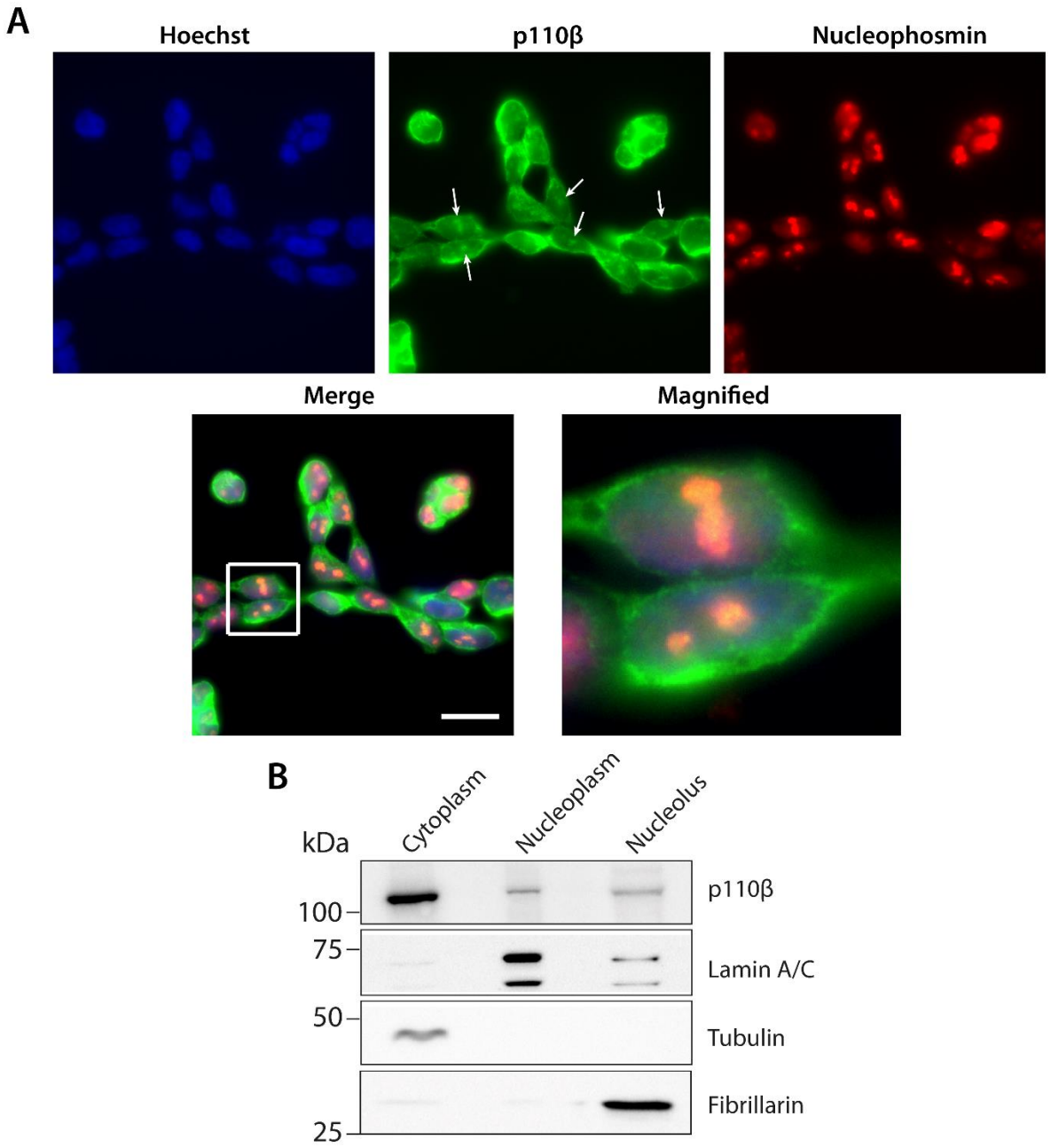

Figure 5.1. Detection of p110β in nucleolus by fractionation and immunostaining of RL95-2 cells. A) Immunostaining of p110β using Abcam anti-p110β antibody, co-stained with anti-Nucleophosmin antibody as a nucleolar marker, and Hoechst DNA stain. Images were taken using epi-fluorescent microscopy at 100 x magnification, exposure time 30 ms, gain 5.0 for p110β. White arrows indicate the colocalisation of p110β with nucleophosmin. The magnified image represents the white square. Scale bar 10 µm. B). Proteins from sub-cellular fractionation of RL95-2 cells were resolved with SDS-PAGE using 40 µg protein from each fraction, and transferred to a nitrocellulose membrane. Western blotting with anti-p110β antibody. Anti-α-Tubulin, -Lamin A/C and -Fibrillarin antibodies were used to verify purity of the fractions. The figure is representative of an experiment performed three times.

To confirm the localisation of PIP3 within RL95-2 cells, immunostaining with an antibody raised against PIP3 was used, in addition to co-staining with anti-nucleolin antibody. Nucleolin is implicated in ribosome biogenesis in the nucleolus (Ginisty et al., 1999). The nucleolin signal was unexpectedly excluded from the nucleoli of the cells, and so a merged image of Hoechst and PIP3 has been added to show the clear nuclear foci of PIP3, as seen in **Figure 5.2**.

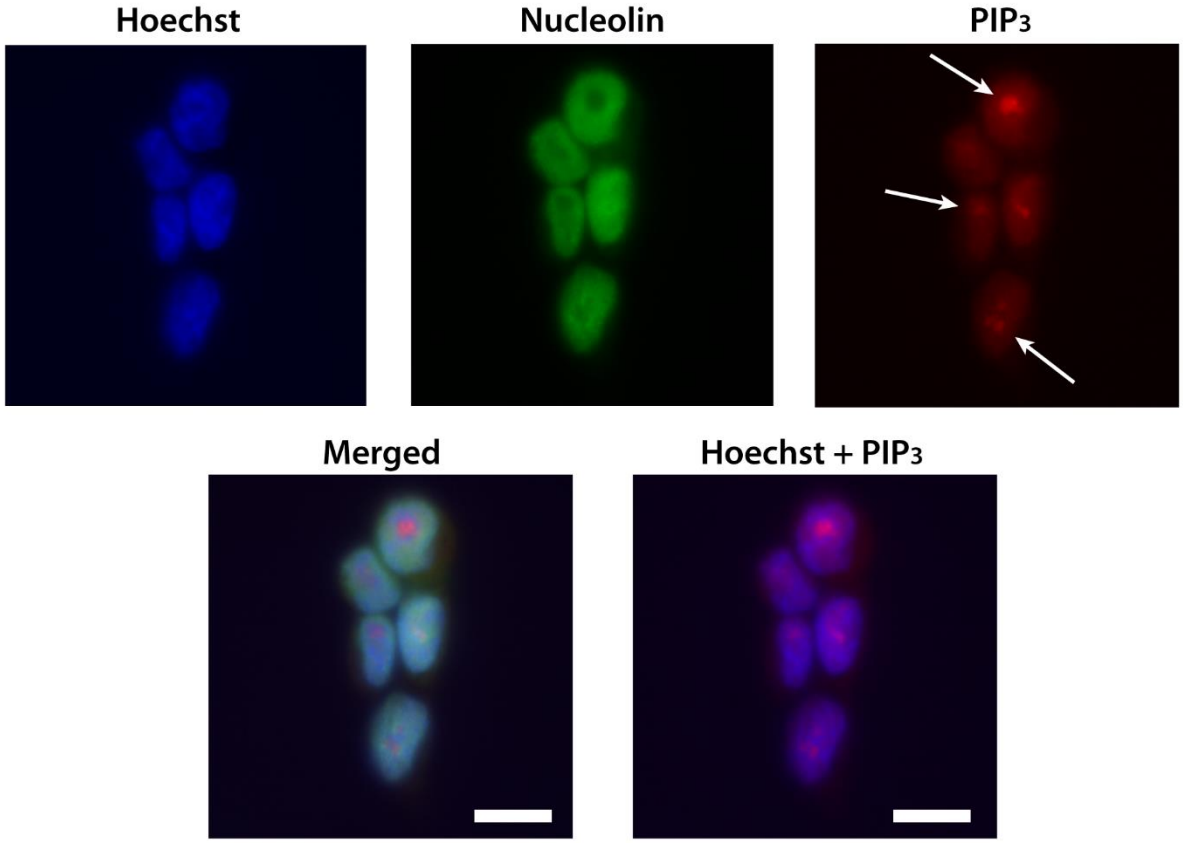

Figure 5.2. Detection of PIP3 within the nucleoli of RL95-2 cells. Immunostaining of RL95-2 cells with anti-PIP3 and anti-nucleolin antibodies as a nucleolar marker. DNA was labelled using Hoechst. Imaging was carried out using epi-fluorescent microscopy at 100x magnification, exposure time 25 sec, gain 6.0 for PIP3. White arrows indicate nuclear foci with PIP3. Scale bar 10 µm.

5.2 Inhibiting p110β with Kin193 reduces transcription of rRNA

This study has demonstrated that p110β is present within the nucleoli of RL95-2 cells. The next task was to understand what its function is within the nucleolus with regard to rRNA transcription. To this end, a selective p110β inhibitor, Kin193, was used to see the effects of this kinase on transcription of 47S rRNA, by RT-qPCR.

To test this, primers matching the 5' external transcribed spacer (ETS) of human 47S rRNA were used in RT-qPCR. This was performed on cDNA made from total RNA isolated from RL95-2 cells. **Figure 5.3** illustrates that the ETS1 primer is placed across the initial cleavage site (01/A' for human, A' for mouse) on the 47S rRNA precursor transcript. This allowed us to specifically target 47S rRNA transcripts, before maturation. Cells were treated with Kin193 for 42 and 72 hours, prior to the observed decrease in the number of cells following p110β inhibition occurring from 72 hours of treatment in RL95-2 cells (*Karlsson et al*., 2016). It is reasonable to assume some time will pass between delayed rRNA transcription and an observable effect on cell proliferation to occur.

The data shown in **Figure 5.4** shows a statistically significant decrease in pre-rRNA transcription of 20% and 16%, 42 and 72 hours respectively after p110β inhibition by Kin193. BMH21, an RNA Pol I inhibitor, was used as a positive control, and as expected, it disrupted all Pol I RNA transcription. The statistical significance was validated using a t-test.

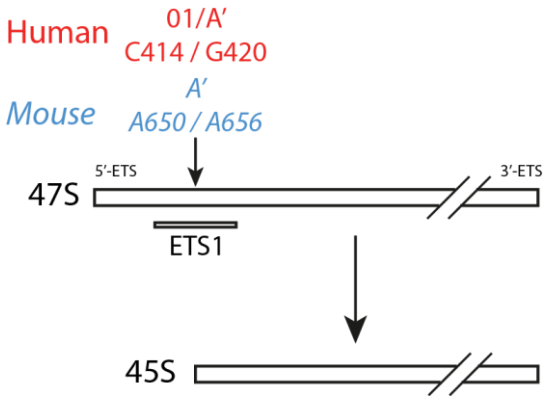

Figure 5.3. Diagram of human and murine 5'-ETS 47S rRNA initial maturation step. The ETS1 primer location is shown to span the initial cleavage site (01/A' for human, A' for mouse). Abbreviations: ETS – external transcribed spacer. The nucleotide numbering corresponds to the GenBank sequences U13369.1 (human rRNA) and BK000964.3 (mouse rRNA).

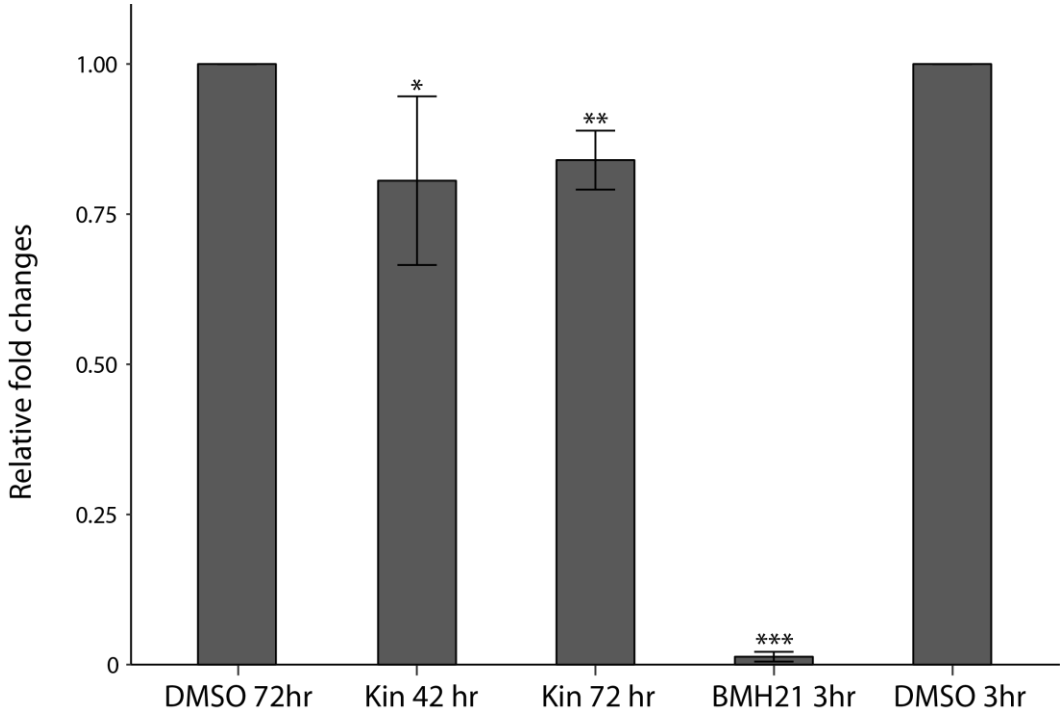

Figure 5.4. Effect of p110β inhibition on rRNA transcription in RL95-2 cells. RL95-2 cells were incubated 24 h after plating with 10 µM p110β inhibitor Kin193 (Kin) for 42 and 72 h or with 1 µM BMH21 for 3 h. The cells were then harvested, RNA was extracted, and cDNA was transcribed. qPCR was run on the cDNA, targeting 47S rRNA transcripts, and normalised to human β-Actin acting as a reference gene. Results were collected from three separate experiments run in triplicates, with both DMSO samples used as negative control, and BMH21 (a RNA polymerase I inhibitor) being used as positive control. Relative fold changes compared to DMSO controls are shown. The symbols (*) used on the graph show the different levels of probability, where * indicates $p<0.05$, ** is $p<0.01$ and *** is $p<0.001$.

5.2.1 Inhibiting p110β with Kin193 reduces RNA levels in acute serum induction in RL95-2 cells

In order to assess the contribution of p110β on nascent RNA transcription, a different method was performed. p110β inhibition by Kin193 was combined with 5-ethynyl uridine (EU) labelling. Incubation of cells with the alkyne-containing EU leads to its incorporation into nascent RNA. Subsequent chemoselective ligation of an azide-containing dye with the alkyne allows for easy detection in a fluorescent microscope (Jao and Salic, 2008). The treatment is simple to perform and can be used in addition to regular antibody staining, and so nucleolin was chosen. Using this method, nascent RNA was detected when it appeared in dark spots in Hoechst signalling, as the nucleolin pattern observed when co-staining with PIP3 persisted in these experiments as well (**Figure 5.2**).

Inhibition of p110β induced a decrease in transcription in actively growing cells (see **Figure 5.4**). This lead to questions regarding conditions where RNA transcription could be monitored acutely. The treatment involved starving the cells in serum-free and low-glucose medium, before giving them a boost of serum for a short period of time. By starving the cells, they are forced to slow down production of ribosomes to conserve energy. Subsequent re-stimulation of the cells should then kickstart rRNA production and reformation of nucleoli (McStay, 2016). To this end, RL95-2 cells underwent starvation for 24 h before receiving a boost of 20% FBS for 30 or 60 min with EU labelling, with and without Kin193. The experiment was performed twice, and the images were chosen to best represent the results. The effects on RNA intensity in serum-free (SF) treated cells compared to control (log) cells can be seen in **Figure 5.5 A**. In the log cells, RNA could be detected clearly not only in the nucleoplasm but also within several nuclear foci, surrounded by nucleolin, observed in a circular pattern. The RNA foci were considered to be nascent rRNA. For the SF-treated cells, however, the signal intensity of rRNA went down overall in the nucleoplasm, and the intensity of the foci showing rRNA decreased substantially. Again, the nucleolin staining in the SF-treated cells seemed to avoid the nucleoli altogether.

When stimulating the cells with FBS for 30 or 60 min (**Figure 5.5 B**), the detected rRNA in the foci seemed to increase in intensity when compared to SF cells, in particular after 60 min of treatment. For cells additionally treated with Kin193, no clear spots of rRNA were visible within the nuclei for either time point post-stimulation. Both the rRNA and nucleolin detected were distributed equally throughout the nuclei, though the signal intensity of nucleolin seems to have decreased in cells treated with Kin193.

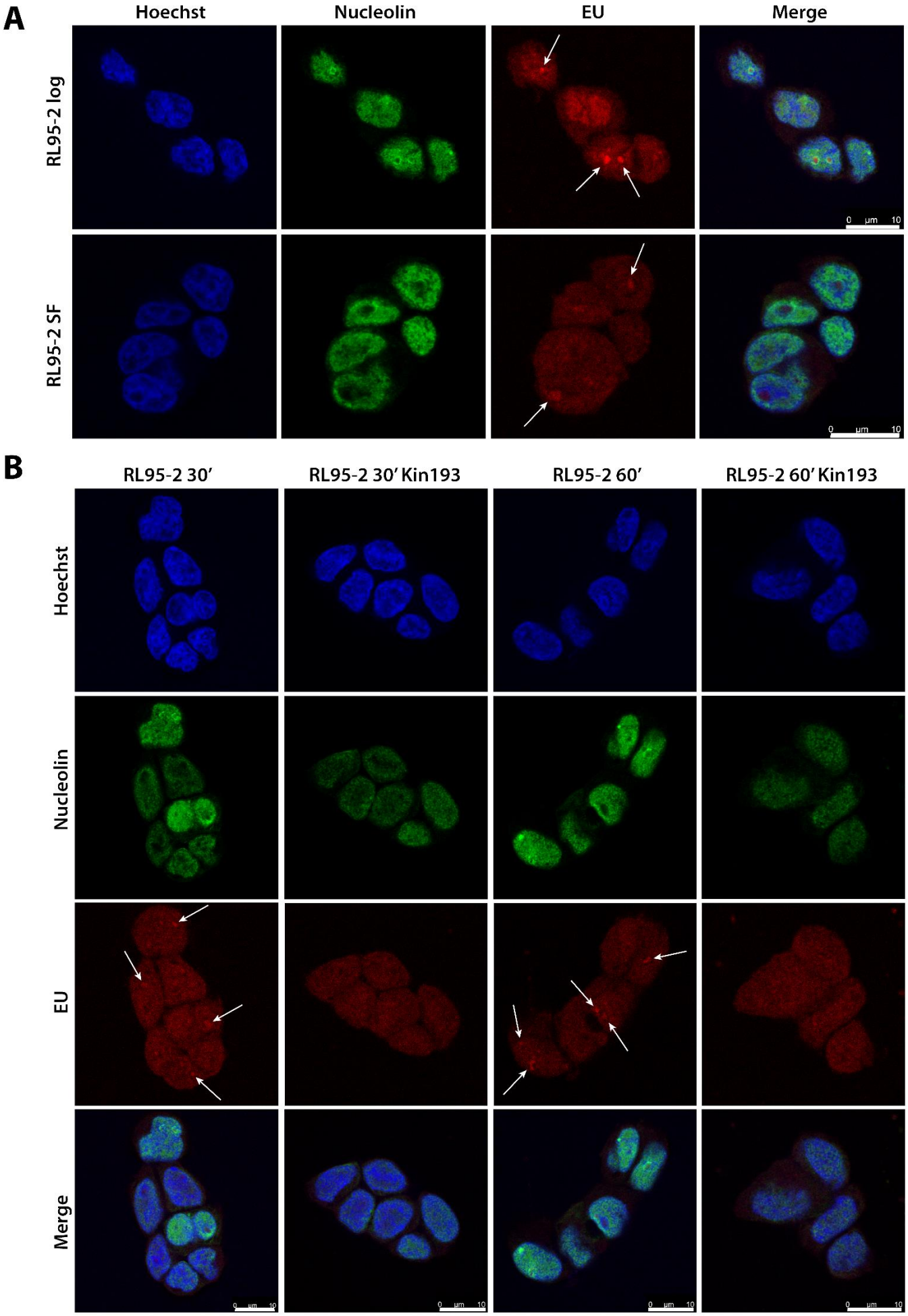
A
Hoechst
Nucleolin
EU
Merge
RL95-2 log
RL95-2 SF
0 µm 10
B
RL95-2 30′
RL95-2 30′ Kin193
RL95-2 60′
RL95-2 60′ Kin193
Hoechst
Nucleolin
EU
Merge

Figure 5.5. Effect of p110β inhibition by Kin193 on RNA intensity 30 and 60 min after reboosting with 20% serum. This caption belongs to the figure on the preceding page. RL95-2 cells were seeded, 500 000 cells per well. A) After 24 h, the growth medium was replaced with serum-free and low-glucose medium, and incubated a further 24 h. B) Cells were then re-stimulated with 20% foetal bovine serum (FBS) for 30 and 60 min, together with EU labelling (total EU treatment time was 30 min), in the presence or absence of Kin193. The slips were co-stained for nucleolin. DNA was stained using Hoechst, and imaged using confocal microscopy. Scale bar 10 µm. The image acquisition parameters were kept the same for all conditions to allow for comparison.

5.3 Inactivating p110β may affect RNA transcription in MEF cells

In addition to studying the human endometrial cancer cell line RL95-2, the effects of the PI3K p110β isoform on RNA transcription was also tested in mouse cells, with a p110β wild type (WT) cell line, and a cell line that had this isoform inactivated (KI). The KI cell line was immortalised with a point mutation, D931A, in the catalytic domain of p110β, which leads to expression of the protein, albeit without its ATP binding capability (Berenjeno *et al.*, 2012).

As with the RL95-2 cells, MEF WT and KI were serum- and glucose-starved for 24 hours, before being stimulated with 20% serum for 30 or 60 min, alongside with EU treatment to specifically target nascent rRNA. The control (log) and serum-free (SF) cells can be seen in in **Figure 5.6**. For both cell lines, several nuclear foci appeared with high signal intensity for EU in log cells. In WT cells, the amount of foci seemed to decrease, albeit marginally, with SF treatment. For KI, the foci disappeared almost altogether, with nearly no clear foci appearing in SF-treated cells. The nucleolin signal in KI log cells was unexpectedly excluded from the nucleoli in about 50% of cells on the slip. The remaining 50% had either some spots of nucleolar signal, or an even, dark distribution of nucleolin throughout the nucleus. In the SF-treated cells, however, nucleolin again appeared nucleolar. Nucleolin signal in WT seemed to change from full coverage within nucleoli in log cells, to being more perinucleolar in SF-treated cells.

The effect of stimulating the cells with serum can be seen in **Figure 5.7**. Unfortunately, during mounting, the slip containing the MEF KI cells 30 min after reboosting with 20% FBS was placed upside-down on the glass slide. Another 5 µl mounting solution and an additional cover slip was carefully placed on top of the slip. The signal intensity of EU 30 min after stimulation in MEF WT was slightly increased, when comparing to WT SF-treated cells. In KI 30 min after stimulation, the signal intensity was very low, with no clear foci, as with SF-treated cells. For both cell lines, several foci become clearer after 60 min of stimulation, when compared to SF.

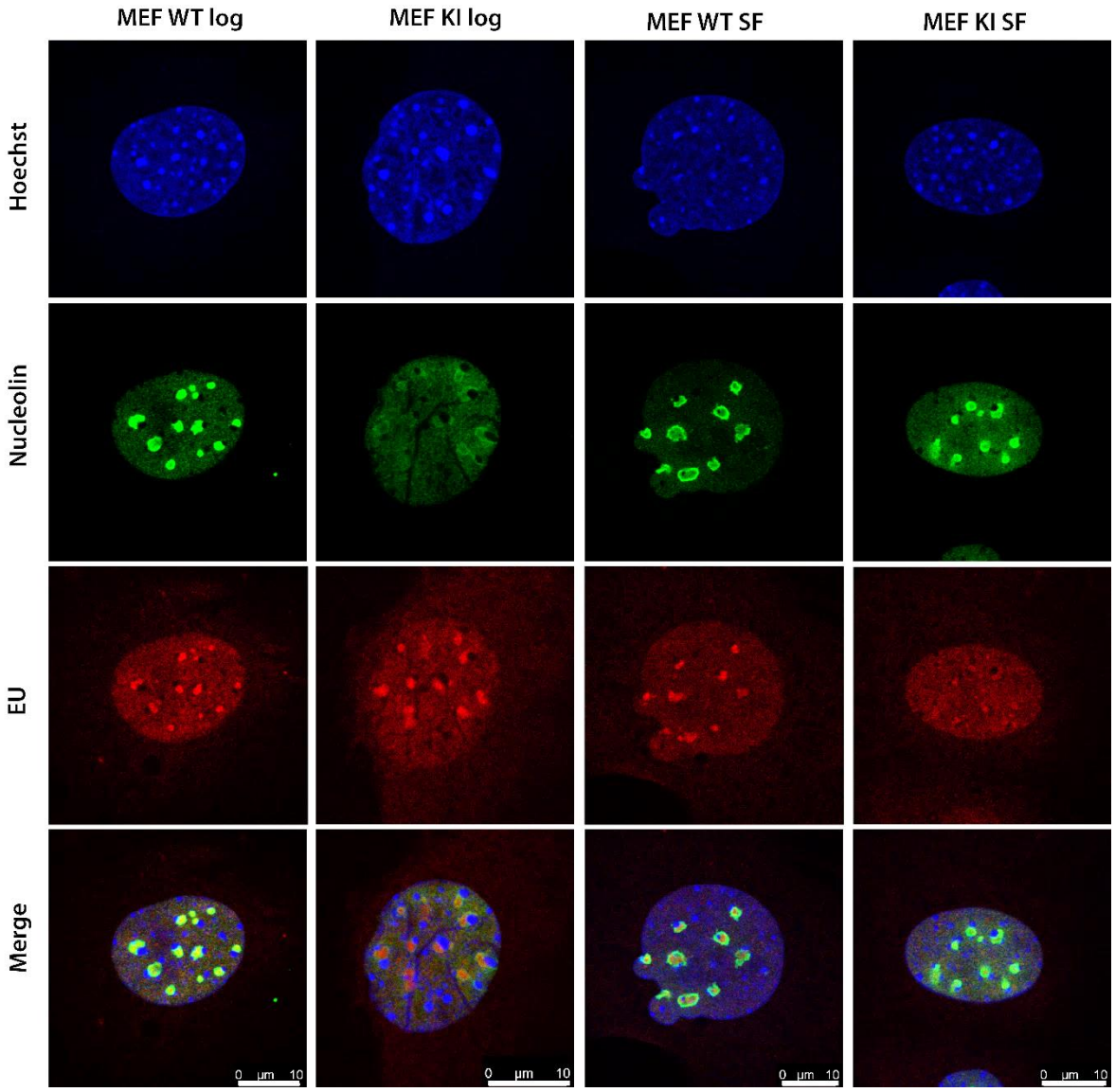

Figure 5.6. Effect of serum on acute RNA transcription in MEF p110β wild type (WT) and kinase inactive (KI). The images are representative of an experiment performed twice. MEF WT and KI cells were plated with 250 000 cells per well and either kept in growth medium throughout the experiment (log) or incubated in serum-free (SF) low glucose medium 24 h after plating, and incubated a further 24 h, together with EU labelling (total EU treatment time was 30 min). The slips were co-stained for nucleolin. DNA was stained using Hoechst, and imaged using confocal microscopy. The image acquisition parameters were kept the same for all conditions to allow for comparison. Scale bar 10 µm.

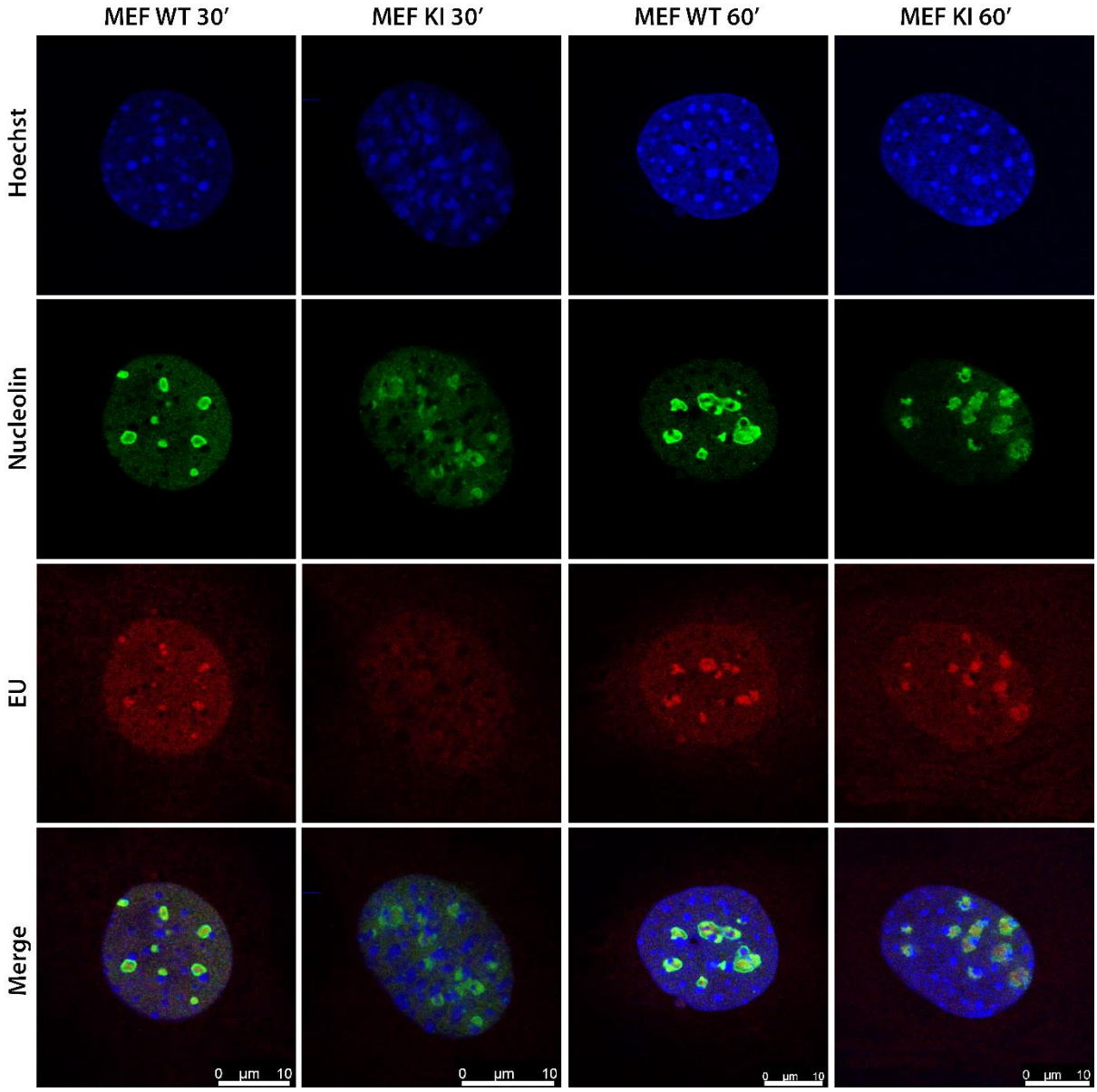

Figure 5.7. Comparing the effect of serum on RNA transcription in MEF WT and KI 30 and 60 min after reboosting with 20% FBS. The images are representative of an experiment performed twice. MEF WT and KI cells were plated, 250 000 cells per well. After 24 h, growth medium was replaced with serum-free (SF) low glucose medium, and incubated a further 24 h, after which cells were stimulated with 20% foetal bovine serum (FBS) for 30 and 60 min, together with EU labelling (total EU treatment time was 30 min). The slips were co-stained with anti-nucleolin antibody. DNA was stained using Hoechst, and imaged using confocal microscopy. The image acquisition parameters were kept the same for all conditions to allow for comparison. Scale bar 10 µm.

To assess 47S rRNA transcription in the MEF cells, RT-qPCR was performed in a similar fashion to the RL95-2 cells, though with mouse ETS primers. The RT-qPCR was performed three times with the same target gene, the murine 47S rRNA transcript, but using different reference genes. Initially, human β-Actin was used, which is almost identical to the murine β-Actin, because our group has previously used it successfully in RT-qPCR using mouse cDNA. Usually, housekeeping genes like GAPDH or parts of the cytoskeleton are reliable as reference genes, because they tend to remain stable and mostly unaffected by experimental factors (Kozera and Rapacz, 2013). However, the serum starvation affected β-Actin too much, as seen in **Figure 5.8 A**, and so a different reference gene was chosen. β2-microglobulin (B2M) is a small protein involved in immune surveillance and modulation, and is expressed at constant levels in many cells (Li *et al.*, 2016). B2M unfortunately didn't work as a reference gene either, shown in **Figure 5.8 B**, where the Cp values varied too much between the samples, and in a different pattern as with human β-Actin (**Figure 5.8 A**).

Analysis of the 47S transcription Cp values was therefore done without including the Cp values for either of the reference genes, as shown in **Figure 5.9**. The data suggests that 47S rRNA transcription is very similar in log samples of both MEF WT and KI. There is a drop in transcription in the KI SF-treated cells however, when compared to the SF-treated WT cells. After stimulating the cells with serum for 30 min, both cell lines have about the same transcription levels. The increase in transcription 60 min after boosting is slightly less in KI when compared to WT.

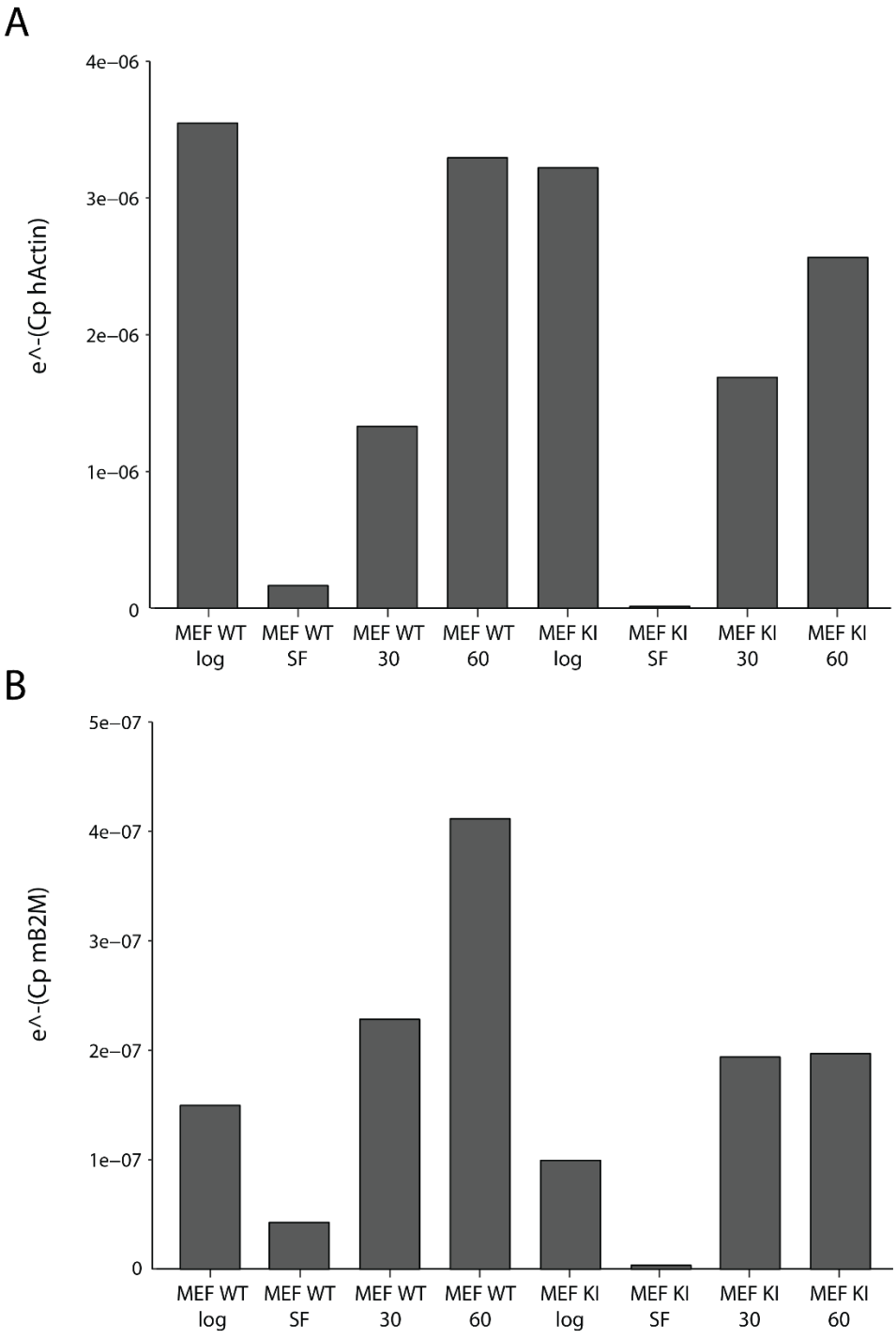

Figure 5.8. Effect of serum starvation and serum induction on different reference genes by qPCR. MEF WT and KI cells were serum-starved with low glucose DMEM for 24 h before being given a boost of 20% foetal bovine serum (FBS) for 30 or 60 min. The cells were then harvested, RNA was extracted, and cDNA was transcribed. qPCR was run on the cDNA, targeting human β-Actin (A) and mouse B2M (B) as reference genes. Only the threshold cycle (Cp) values, normalised to the respective primer efficiency value from the reference genes are shown. e^-(Cp X) indicates that the Cp values are normalised to the primer efficiency or the experiment. For hβ-Actin, primer efficiency was 1.96, for mB2M it was 1.932.

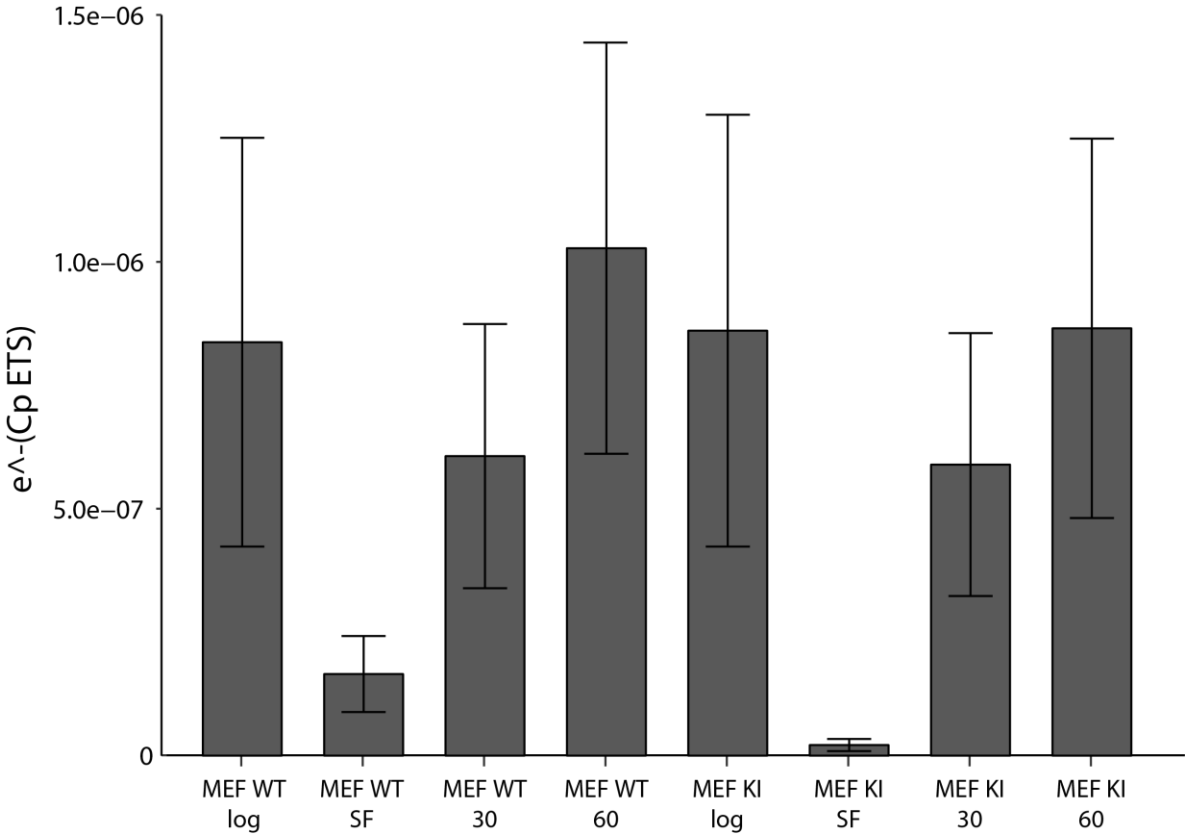

5.9. Effects of restimulating MEF WT/KI cells with 20% FBS on pre-rRNA 47S transcription with qPCR. MEF WT and KI cells were serum-starved with low glucose DMEM for 24 h before being given a boost of 20% foetal bovine serum (FBS) for 30 or 60 min. The cells were then harvested, RNA was extracted, and cDNA was transcribed. qPCR was run on the cDNA, targeting 47S rRNA transcripts. The results are collected from two individual experiments. Only the threshold cycle (Cp) values, normalised to the primer efficiency value from the ETS gene is shown. e^-(CpETS) indicates that the Cp were normalised to the primer efficiency of each experiment, then the average was calculated. ETS primer efficiency for experiment 1: 1.91, experiment 2: 1.96.

5.4 GST-PARP1 binds PIP3

PPIn act by binding and recruiting proteins. Previously, our group has identified PARP1 as a PIP3 binding protein by mass spectrometry of PIP3 lipid pull-down from nuclear extracts (Mazloumi Gavgani *et al.*, 2017). In the same study, PARP1 and PIP3 were shown to colocalise in the nucleoli, by immunofluorescence staining. Furthermore, a direct *in vitro* interaction of PARP1 with PPIn was shown. However, which part of the protein is involved in PPIn-interaction is hitherto unknown. To discover this, GST-fused fragments of PARP1 were expressed and purified, and a lipid overlay assay was performed to assess the lipid-binding properties.

5.4.1 Expression and purification of GST-PARP1 fragments

To discover the binding interaction to PPIn, PARP1 was expressed as five separate fragments, obtained from Prof. Michael O. Hottiger, University of Zurich. A diagram of the relevant domains can be seen in figure **5.10 A**. The first fragment contains the first 214 amino acids, which include the two zinc-finger domains, and parts of the first of two nuclear localisation signals (NLS). This fragment is also the main part of the DNA-binding domain. Fragment 2 covers the second NLS motif, and ends before the beginning of the BRCA1 C-terminus like (BRCT) domain. It also has 5 helices, 2 β-turns and 4 β-strands. Fragment 3 contains the automodification domain, thought to be part of protein-protein interaction (Tao *et al.*, 2009), though large parts of the secondary structure remains unknown for this portion of the protein. Fragment 4 contains no domains of interest, and fragment 5 is the rest of the protein, containing an α-helical domain and the catalytic domain.

The expression and purification of GST-PARP1 fragments was monitored by SDS-PAGE, see **Figure 5.10 B**-**F**. The protein eluates are pure in all fragments, except for some impurity observed for fragment 1 (**Figure 5.10 B**), which is likely some co-purified protein. For fragments 1, 3, 4 and 5, a band corresponding to the size of GST can clearly be seen at around 25 kDa. The expression levels varied slightly between the fragments, with the greatest difference in fragment 2.

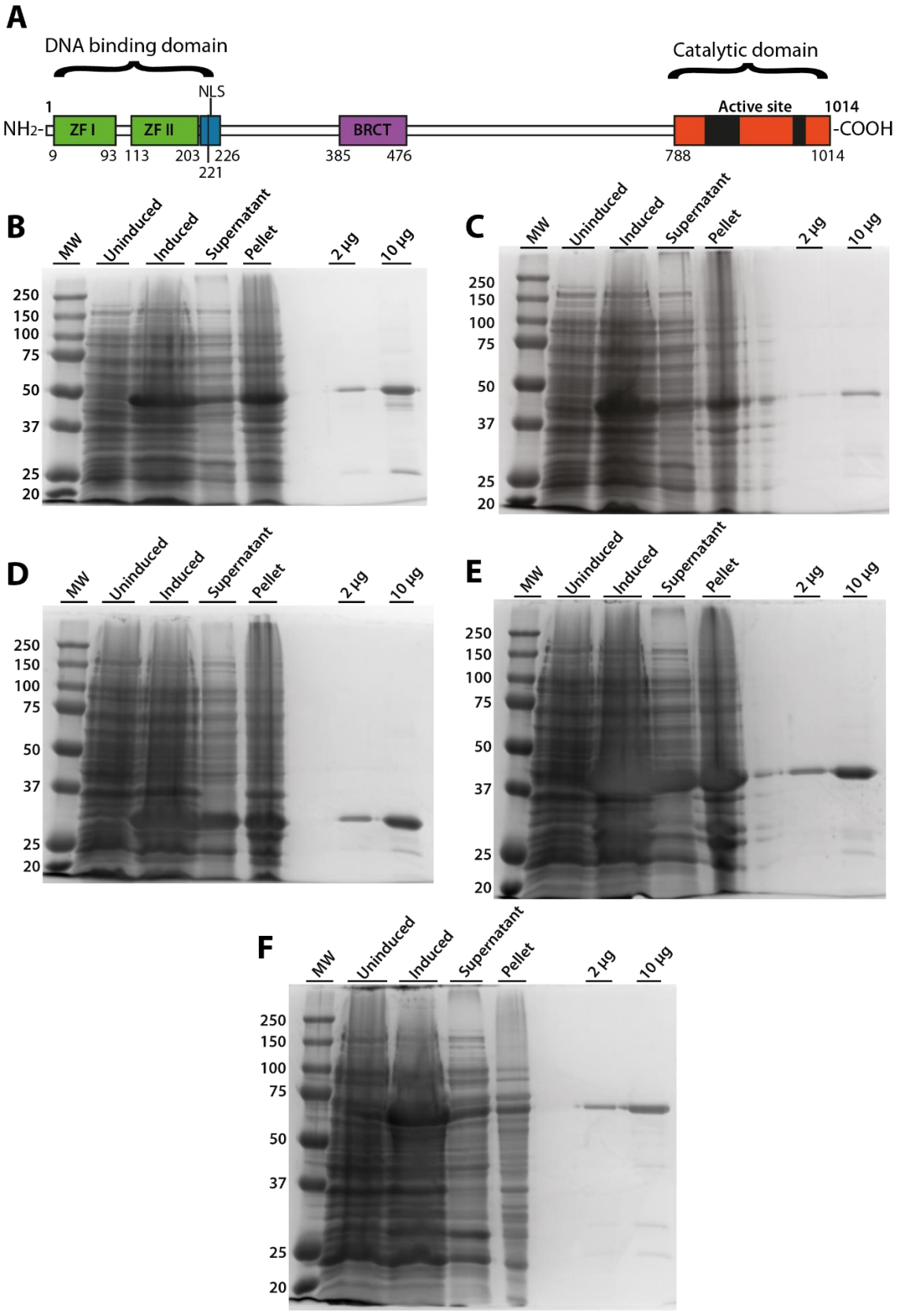
A
DNA binding domain
Catalytic domain
NLS
1
NH2-
ZF I
ZF II
BRCT
Active site
1014
-COOH
9
93
113
203
226
221
385
476
788
1014
B
C
D
E
F
MW
Uninduced
Induced
Supernatant
Pellet
2 µg
10 µg
250
150
100
75
50
37
25
20

Figure 5.10. Purification of GST-PARP1 fragments. This caption belongs to the figure on the preceding page. A) Diagram of PARP1 domains. The catalytic and DNA binding domains are shown with brackets. Domains and secondary structure information were collected from UniProtKB for Human PARP1; P09874. B-F) GST-PARP1 was expressed using BL-21 Codon Plus® (DE3)-RIL competent cells, and soluble protein was purified using glutathione-sepharose beads. The Bradford protein concentration assay was utilized to determine protein concentration. The following was loaded onto SDS-PAGE; 7 µl Precision Plus Protein™ Dual Color standard from BioRad, 15 µl uninduced culture, induced culture with OD corresponding to uninduced, 5 µl induced supernatant, 4 µl bacterial pellet, and lastly, 2 and 10 µg of purified protein. GST-PARP1 fragments 1-5 (B-F respectively) are shown, the amino acid sequence being the following: fragment 1: 1-214, fragment 2: 215-371, fragment 3: 477-524, fragment 4: 525-656, fragment 5: 657-1014. GST has a MW of 25 kDa. Abbreviations: ZF (I and II) – Zinc Finger, NLS – Nuclear Localization Signal, BRCT – BRCA1 C-Terminus like domain.

5.4.2 GST-PARP1 fragments 2 and 3 bind PIP3

Lipid binding properties of each of the GST-PARP1 fragments were assessed using PIP strips from Echelon. Each strip is spotted with 100 pmol of each of the seven PPIns and other lipids, as indicated in **Figure 5.11 A**. Purified protein from each fragment elution was incubated on the membranes, and visualized with ECL. The results can be seen in **Figure 5.11 B**, with red arrows pointing to the relevant binding of fragments 2 and 3 to PIP3. This is not the only PPIn the fragments bind, however. Fragments 1, 2 and 3 all bind a variety of lipids, with different interaction patterns. Fragment 3 also binds very strongly to PtdIns(3,5)P_2 and PA. Fragments 4 and 5 didn't seem to bind any lipids on the membranes.

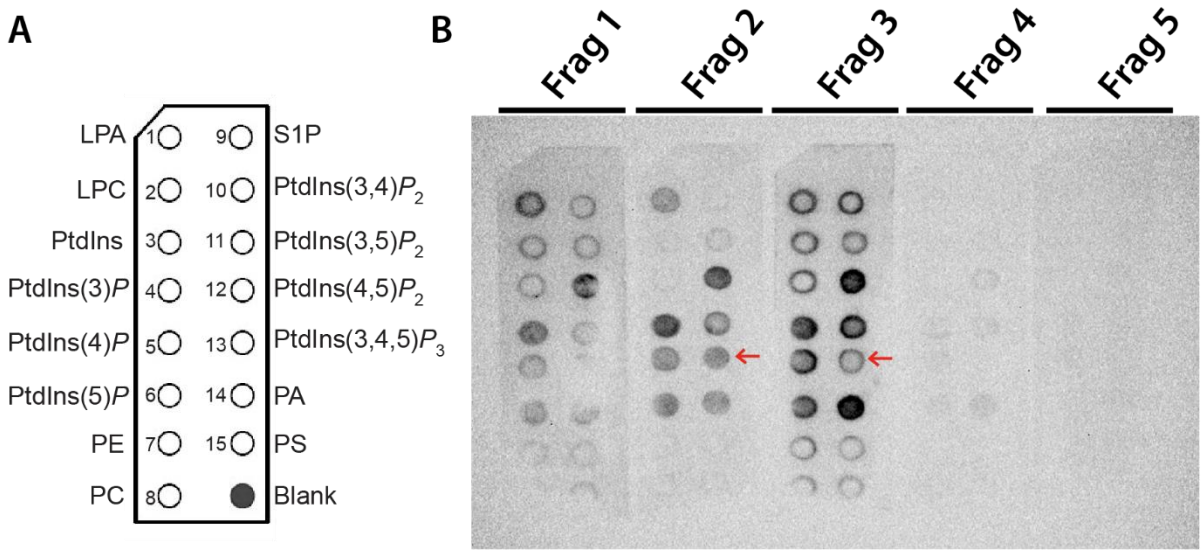

Figure 5.11. Lipid overlay assay of GST-PARP1 fragments 1-5 to demonstrate lipid binding properties. A) Illustration of PIP strips. Each strip is spotted with 100 pmol of the following lipids: Lysophosphatidic acid (LPA), Lysophosphocholine (LPC), Phosphatidylinositol (PtdIns), Phosphatidylinositol(3)phosphate (PtdIns(3)*P*), Phosphatidylinositol(4)phosphate (PtdIns(4)*P*), Phosphatidylinositol (5) phosphate (PtdIns(5)*P*), Phosphatidylethanolamine (PE), Phosphatidylcholine (PC), Sphingosine 1-Phosphate (S1P), Phosphatidylinositol(3,4) bisphosphate (PtdIns(3,4)P_2) , Phosphatidylinositol(3,5)bisphosphate (PtdIns(3,5)P_2), Phosphatidylinositol(4,5)bisphosphate (PtdIns(4,5)P_2), Phosphatidylinositol(3,4,5) trisphosphate (PtdIns(3,4,5)P_3), Phosphatidic acid (PA) and Phosphatidylserine (PS). B) GST-PARP1 DNA sequence was expressed as five fragments as the following (in amino acid sequence): fragment 1: 1-214, fragment 2: 215-371, fragment 3: 477-524, fragment 4: 525-656, fragment 5: 657-1014. PIP strips were used to demonstrate the lipid binding properties of PARP1 fragments. 0.5 µg/mL purified GST-PARP1 fragments 1-5 (Frag 1-5) was added to the lipid blots and incubated for 1 h at RT. Visualization was done by adding anti-GST conjugated HRP and imaging using chemiluminescence.

6. Discussion

The PI3K pathway has been studied extensively, however each new discovery is accompanied by more questions. With so many components and possible cellular outcomes, how does it all work together? This problem escalates when taking into account the different PI3K isoforms being implicated. Most of the research performed on this pathway has been devoted to the Class I PI3K p110α isoform, due to frequent mutations found in the p110α-coding *PIK3CA* gene in many human cancers. PI3K p110β has received less attention but has been observed to be tumorigenic when overexpressed in its wild type form, without the need for an activating mutation (Kang *et al.*, 2006). However, the mechanism with which p110β promotes cell proliferation and tumour growth is still unknown.

Our group has compiled substantial evidence to suggest the existence of a link between p110β and the nucleolus. Therefore, discovering the nucleolar function of p110β was the focus of this thesis. p110β is overexpressed in some cancers, including endometrial cancer (Karlsson *et al.*, 2017), and tumorigenesis has been shown to be dependent on its lipid kinase activity (Wee *et al.*, 2008). p110β has been shown to localise in the nucleus and nucleolus of human breast cancer cells, and inhibition of this particular isoform has been linked to decreased cell proliferation (Karlsson *et al.*, 2017). Among other functions, the nucleolus is responsible for production of ribosomes, which are vital in cell proliferation (Derenzini *et al.*, 2017). Since p110β kinase activity is seen in non-cancerous cells in addition to cancer cells, it is likely involved in normal nucleolar function. It would be interesting to test if overexpression of this isoform leads to cancerous cell division as a result of increased rRNA production to satisfy the need for more ribosomes. The results of this thesis indeed suggest that p110β has a positive effect on rRNA transcription in the PTEN-negative endometrial cancer cell line RL95-2. However, the underlying molecular mechanism could not be determined within this study. PARP1, involved in DNA repair and localised in nucleoli, was found to be a PIP3 effector protein as a result of PIP3 lipid pull-down from nuclear extracts of HeLa cells (Mazloumi Gavgani *et al.*, 2017). The results of this study confirm that fragments of GST-PARP1 bind a variety of PPIn, including PIP3. Further research is required to assess whether PARP1 is regulated by PIP3 in the nucleolus.

6.1 p110β and PIP3 are nucleolar in RL95-2 cells

During the course of this study, p110β and its lipid product PIP3 were shown to localise in the nucleoli of the endometrial cancer cell line RL95-2. This is consistent with previous studies from our group validating the localisation of p110β in AU565 cells (Karlsson *et al.*, 2016) and HeLa cells (unpublished paper in: (Mazloumi Gavgani *et al.*, 2017)). In addition, high grade endometrial tumours correlate with high nuclear p110β levels (Mazloumi Gavgani *et al.*, 2017). This would suggest that p110β contributes to development of this type of tumour in a nuclear and perhaps also in a nucleolar dependent manner.

The localisation of p110β in the nucleolus was confirmed by immunostaining and cell fractionation following western immunoblotting. When assessing the purity of the sub-cellular fractions of RL95-2, Lamin A/C was used to confirm the purity of the nucleoplasmic fraction. However, this protein is also present in the nucleoli of these cells. This is consistent with previous findings, which demonstrate that A-type lamins interact with several nucleolar proteins (Legartova *et al.*, 2014). Finding a pure nucleoplasmic marker that is not also nucleolar turned out to be a challenge. One example could be to try one of the nucleoporins. These proteins assemble into the nuclear pore complexes, found on the nuclear envelope (Nofrini *et al.*, 2016). Antibodies for various nucleoporins have previously been used as markers for the nuclear membrane in western blotting and immunofluorescent staining (Lizotte *et al.*, 2005; Huang *et al.*, 2013). One issue with using such a marker, however, could be contamination in the cytoplasmic fraction, due to parts of the nuclear membrane being transferred to the cytoplasm fraction during the fractionation procedure. Also, nucleoporins do not represent the entire nucleoplasm, only the envelope.

The specificity of the p110β and PIP3 antibodies used in this study have been validated by our group. siRNA knock down following western blotting and staining with p110β antibody validated the specificity of the antibodies used in this thesis. The specificity of the PIP3 antibody was also validated by competition assays using free lipids (PtdIns3*P*, Ptdins(3,4)*P2* and PIP3). In addition, the nucleolar presence of PIP3 has been confirmed by liquid chromatography–mass spectrometry (LCMS) and a lipid blot (Mazloumi Gavgani *et al.*, 2017). Our group has regularly used an anti-nucleolin antibody as a nucleolar marker, as it is an abundant protein in this sub-nuclear structure. However in RL95-2 cells, nucleolin, which is known to take part in rDNA transcription and rRNA maturation (Ginisty *et al.*, 1999), was not

detected in the nucleoli of these cells when using immunofluorescent staining. NPM, on the other hand, was clearly seen as being nucleolar in the same cell line (**Figure 5.1**). Consistently, the nucleolin signal appeared to be excluded from the nucleoli, instead appearing rather strongly in the nucleoplasm, or as circles or in caps around nucleoli. The nucleolin pattern was, for the most part, not found in the MEF WT or KI cells, which are PTEN-positive and don't harbour a hyperactive PI3K pathway, which were stained using the same antibody. However, determining if the cause of this unexpected pattern was due to the antibody or the cells remains unknown. It is also possible that it is instead located in the granular component or dense fibrillar component. In this case, it could be verified by using a granular component marker, like fibrillarin. To our knowledge, the use of this antibody for staining this cell line has not previously been described, and so there could be some underlying mechanism that displaces nucleolin. Indeed, the localisation of nucleolin may be dependent on the expression of different isoforms of PTEN (Liang *et al.*, 2017). It could also be that PTEN-deficiency leads to unstable nucleolin in the nucleolus. However, this signal pattern was not found in a study that used nucleolin as a marker in both PTEN-positive and negative human prostate cancer cell lines. Here, the pattern was unchanged between the cells (PC3 or LNCaP cell lines) (Li *et al.*, 2014). In the same paper, HeLa cells were transfected with short hairpin RNA against PTEN, but the nucleolin pattern remained unchanged.

6.2 Inhibition of p110β leads to decreased rRNA transcription

Since the best-known processes within nucleoli are rRNA transcription and maturation (Pederson, 2011), and ribosome assembly, p110β and PIP3 may participate in one or many of these processes. Investigating the effects of p110β on rRNA transcription has not yielded any published research, to our knowledge, and so these findings are novel and lead to more questions regarding the detailed mechanism with which p110β and PIP3 may be involved. Indeed, Drakas *et al*. have observed that a Class I PI3K (likely p110β) can activate rDNA transcription by interacting with, and phosphorylating UBF (Drakas *et al.*, 2004). They did not study the lipid kinase capability of this p110 isoform, however. UBF is a transcription factor involved in rRNA transcription, as part of the pre-initiation complex (Kwon and Green, 1994). Possible interaction between UBF and p110β strengthen the hypothesis that p110β is involved in ribosome biogenesis. This could be tested by performing immunoprecipitation (IP) using a specific antibody against p110β or UBF, to see if they interact.

Both chronic and acute rRNA expression in RL95-2 was assessed by RT-qPCR and EU labelling respectively. Acute rRNA transcription was monitored by starving the cells to synchronise their growth and subsequently stimulating them with serum for a short period of time. As opposed to this, for RT-qPCR experiments RNA was isolated from actively growing cells. The findings of this thesis demonstrate a statistically significant decrease in rRNA transcription in RL95-2 cells upon inhibition of p110β by Kin193. Kin193 selectively inhibits p110β and the PI3K/Akt pathway (Edgar *et al.*, 2010; Jamieson *et al.*, 2011), and our group has shown that inhibition of this kinase leads to a decrease in the nuclear PIP3 pool in these cells (Mazloumi Gavgani *et al.*, 2017). Also, Kin193 has been observed to inhibit tumour growth in PTEN-negative mouse tumour cells (Ni *et al.*, 2012). Ni *et al*. accentuate that Kin193 could be used as a potential anti-cancer drug. Ideally, Kin193 would disrupt the effects of p110β and the PI3K/Akt pathway, leading to less overall ribosome production, resulting in decreased cell proliferation.

Our group has shown that p110β protein and mRNA levels (for *PIK3CB*) increase in EC cell lines, including RL95-2, which has high nuclear p110β (Mazloumi Gavgani *et al.*, 2017). This would indicate that they are good candidates for selective p110β inhibition. However, the decrease in rRNA transcription brought on by p110β inhibition was only 20%. p110β inhibition may prevent the production of new PIP3, but it does not take into account pre-existing PIP3 present in the cells. This assumption is based on PIP3 being produced in the nucleolus by p110β. However, at this stage we cannot rule out that PIP3 can potentially be made elsewhere and translocate to the nucleoli. RL95-2 cells are PTEN-deficient, meaning that PIP3 catabolism is slow to begin with. It could also be that the inhibitor doesn't have the capacity to fully enter the nucleolar p110β pool, thus lowering its potential power of inhibition. Treating the cells for a longer period might show further reduction in 47S rRNA transcription than is seen after 72 hours of treatment. Also, the nuclear PIP3 pool has been shown to be resistant toward metabolisation by PTEN in mouse Swiss 3T3 cells (Lindsay *et al.*, 2006), and it could be that this pool is instead metabolised by a 5-phosphatase like SHIP2. This has since been disputed however, with others claiming that treatment with PTEN help regulate the nuclear PIP3 pool in PC12 cells, by disrupting PIP3 interaction with NPM and Akt (Kwon *et al.*, 2010).

Even though the catalytic activity of p110β is through lipid phosphorylation, speculations around other properties of the protein have come to light. This becomes evident when considering that inhibition of p110β leads to decreased cell proliferation (Karlsson *et al.*, 2017),

whereas p110β knock-down leads to apoptosis in endometrial cancer cells (An *et al.*, 2007). p110β has been associated with kinase-independent functions including activity within autophagy by sensing growth factor availability (Dou *et al.*, 2013), metabolic regulation and glucose homeostasis (Jia *et al.*, 2008), and as a scaffolding protein in insulin signalling (Jia *et al.*, 2008). Interestingly, Kumar *et al*. have proposed a kinase-independent function for p110β in DNA double strand break repair (Kumar *et al.*, 2010). Taken together, these findings suggest that the role of p110β in the nucleus and perhaps nucleolus might be kinase-independent, or multifunctional.

There seems to be some differences when comparing the effects of inhibiting p110β with Kin193 in RL95-2 cells to the inactivating mutation present in the MEF KI cells. Inhibiting p110β using the drug seems more effective than the mutation, with regard to rRNA transcription. When comparing MEF WT to KI in rRNA transcription, both chronic (RT-qPCR) and acute (EU labelling), the effect of the mutation in KI seems minimal. This would suggest that there is no inherent difference between MEF WT and KI regarding this process. Indeed, the only difference between the WT and KI cell lines is an inactivating mutation present in the KI cells; a single point mutation from an aspartic acid residue to alanine (D391A) which is involved in ATP binding, by stabilizing the enzyme structure. It could be that the catalytic mutant is still partially active in some cells. This could be due to how the ATP kinase mechanism of a phosphotransferase works, which is similar for many kinases. In this mechanism, the most important conserved amino acid in ATP binding is a lysine residue, along with other charged amino acids like glutamate and aspartate (Gibbs and Zoller, 1991; Wang and Cole, 2014). Perhaps the structure is disrupted, but still partially functioning with the mutation. In another study, where p110β was inactivated with a point mutation in the conserved lysine residue (K805R), Marqués *et al*. saw a reduction in phosphorylated Akt, a downstream target of p110β (Marques *et al.*, 2008). It could also simply be that the MEF model is not suited for studying rRNA transcription in the manner performed in this study. Instead, a knock-out cell line could be used.

We observed additional problems with RT-qPCR regarding finding a suitable housekeeping gene to be used as a normaliser for growth arrested cells. Cell treatment involved starvation, which has an impact on most pathways and processes in the cell. A study from 2016, which assessed the effects of serum starvation on a variety of housekeeping genes in colon adenocarcinoma cell lines, found that both β-Actin and B2M, which were used in our study,

were unstable when afflicted with starvation and re-stimulation (Krzystek-Korpacka *et al.*, 2016). The authors concluded this due to transcription levels being significantly up-regulated upon re-supplementation of serum, for both genes. In their study, they concluded that the most stable gene to be used in this treatment was ribosomal protein large P0 (RPLP0), a component of the 60S ribosomal subunit. However, we would prefer not to use a nucleolar or ribosomal related protein in this experiment. Indeed, the results of this thesis indicate that both β-Actin and B2M varied so much in the different cell conditions, that they were deemed unsuitable to be used as reference genes.

The levels of B2M mRNA expression vary in a different pattern compared to human β-actin and 47S rRNA transcription in MEF WT/KI cells. Here, transcription in KI is lower overall, for all cell conditions, compared to WT. This could indicate another purpose for p110β in the nucleolus. After all, this subnuclear structure is not only involved in rRNA transcription, but also other functions, such as stress response and cell cycle progression (Pederson, 2011; Ogawa and Baserga, 2017). Instead of solely being involved in rRNA transcription, p110β and PIP3 could instead have a different nucleolar purpose, maybe in general transcription or processing.

6.3 *In vitro* binding of PARP1 to PIP3

Our group has shown direct interaction between PARP1 and PIP3 (Mazloumi Gavgani *et al.*, 2017), the lipid product of p110β. PAPR1 is an interesting candidate, because it is found in the nucleolus (Meder *et al.*, 2005), and contains 3 KR-motifs throughout its sequence (see **Appendix 1**). This thesis shows that fragments 2 and 3 of expressed and purified GST-PARP1 bind PIP3. Fragment 2 contains an NLS motif and one KR-motif, and fragment 3 contains one KR-motif. If the interaction between PARP1 and PIP3 changes the activity of PARP1, this could have implications. PARP1 has been linked to ribosomal biogenesis in Drosophila nucleoli (Boamah *et al.*, 2012), and PARP1 and PARP2 have been shown to interact with NPM (Meder *et al.*, 2005).

Among other roles, PARP1 is involved in single stranded break (SSB) repair of DNA (Satoh and Lindahl, 1992). Disrupting the SSB repair pathway will lead to an accumulation of double strand breaks (DSB), which need to be repaired by a DSB repair mechanism like DNA homologous repair (HR). Inhibiting PARP will thus lead to a build-up of DSB in HR-deficient cells, for example BRCA1/2-mutated cells. The result of this is toxic, and leads to apoptosis, an effect known as synthetic lethality (Farmer *et al.*, 2005). There already exists a PARP-

inhibitor in clinical trials, though it is restricted to patients with BRCA1/2 mutations. It has been shown, however, that PTEN-deficient tumours are sensitized to PARP-inhibitors in other cancers as well, including endometrial cancer (Shen *et al.*, 2013; Koppensteiner *et al.*, 2014). This was also demonstrated by Dedes *et al*. who treated EC cells with PARP and PI3K inhibitors in concert, and concluded that the cells treated with a pan-PI3K inhibitor became sensitized to PARP inhibitors (Dedes *et al.*, 2010). Also, inhibition of PI3K by BKM-120 has been shown to impair BRCA1/2 mRNA transcription, leading to HR repair dysfunction (Ibrahim *et al.*, 2012). Though the inhibitors used in these studies were pan-PI3K inhibitors, it would be interesting to see if similar results could be reproduced using a p110β specific inhibitor. Perhaps limiting the supply of PIP3 by inhibiting p110β could impede the effects of PARP1, thus leading to sensitivity to PARP1 inhibition, and subsequent apoptosis by synthetic lethality.

When expressing GST-PARP1, one fragment was not included. However, this fragment contains no KR-motifs or other PI-binding domains and may not be involved in PPIn binding. The fragment is currently being characterised by our group. The PPIn binding pattern of the different fragments vary quite substantially (see **Figure 5.11**). Fragments 1, 2 and 3 bind lipids, and fragment 3 binds quite strongly to PtdIns(3,5)P_2, PtdIns(4,5)P_2 and PA. It is known that PtdIns(4,5)P_2 is found in the nucleolus, and that it promotes Pol I transcription through interaction with UBF and fibrillarin (Yildirim *et al.*, 2013). Since this is a precursor to PIP3, there might exist an interplay between the two lipids with PARP1.

Our group has expressed fragment 3 of GST-PARP1 for use in interaction studies in nuclear magnetic resonance (NMR) spectroscopy. Preliminary NMR results further confirm that fragment 3 does indeed bind PIP3, and the amino acids involved include the polybasic region KR-motif, as seen in **Appendix 1.** This fragment was chosen as a test because it is the smallest fragment, hence more amenable for NMR studies, and binds many PPIn, including PIP3. These results were analysed from HSQC spectra, and concluded based on an observation of displaced peaks when comparing spectra from free PARP1 versus PARP1 bound to PIP3. The amino acids thought to be involved in PIP3 binding are highlighted in red in **Appendix 1**. Three KR-motifs have been found within the sequence of PARP1, all shown in blue in the same appendix. It would be interesting to see if the other fragments show similar results.

6.4 Is the nucleolar role of p110β linked to tumorigenesis?

Changes in nucleolar structure and function have been shown to correlate with cancer, with larger nucleoli being linked to increased Pol I transcription activity (Farley *et al.*, 2015). Indeed, a growing tumour is in high demand of protein translation, and so all aspects of amplified ribosome biogenesis would benefit the cancer cells. p110β mainly functions as a lipid kinase, and oncogenic transformation in PTEN-negative cells has been shown to depend on this activity (Wee *et al.*, 2008). It could be that the increase in PIP3 by p110β activity in the nucleolus promotes tumorigenesis in endometrial cells through up-regulation of ribosome biogenesis. Increased ribosome production has also been linked to development of endometriosis, a disease causing abnormal growth in the endometrium and infertility, and is a precursor to uterine cancers (Chang *et al.*, 2016). A correlation between increased activity of the PI3K/Akt pathway and endometriosis has been established (Yin *et al.*, 2012). Activation of the pathway prevents endometriotic stromal cells from undergoing decidualization, which is necessary for pregnancy (Gellersen *et al.*, 2007). However, this study did not look into which isoform was involved. With the findings of this thesis, we suggest that it is p110β that is implicated here, and that increased p110β activity promotes initiation of tumorigenic transformation.

Taken together, the results of this thesis on p110β indicate that Kin193 could be further pursued as a potential anti-cancer drug in PTEN-negative endometrioid endometrial cancers. Inhibiting or inactivating the lipid-kinase activity of p110β seemingly influences the nucleoli of both human and mouse cells, though details are hard to determine. Whether or not the mechanism with which p110β is involved in rRNA transcription and ribosome biogenesis is kinase-dependent is still unknown. Future experiments might include longer treatment of cells with Kin193, to see if there is a continued decrease in 47S transcription after 72 hours. One could also try mutating a different amino acid residue within p110β, to further disrupt ATP binding. As discussed above, the hypothetical interaction between UBF and p110β could be tested by IP experiments and the role of p110β/PIP3 in rRNA transcription can be tested through chromatin IP (ChIP) experiments. Another idea could be to use small interfering RNA to silence the p110β gene. This has been attempted by our group, though preliminary results lead to cells dying.

The binding of PARP1 to PIP3 leads to questions regarding further regulation of PARP1 by p110β. Is there a deeper link between p110β, PIP3 and PARP1? DNA damage can occur from vast amounts of sources, both internal and external. The nucleolus has been shown to house several proteins involved in not only ribosome biogenesis, but also DNA-binding proteins, and DNA-repair proteins (Ogawa and Baserga, 2017). With PARP1's presence in the nucleolus and involvement in DNA repair, it is possible that some crosstalk occurs between p110β/PIP3 and PARP1 to regulate this function. Further investigation into this theory might strengthen the idea of using a specific p110β inhibitor together with PARP1 inhibitors as a treatment option for patients with PTEN-negative endometrial cancers.

7. References

Ahn, J. Y. *et al.* (2005) 'Nucleophosmin/B23, a nuclear PI(3,4,5)P3 receptor, mediates the antiapoptotic actions of NGF by inhibiting CAD', *Molecular Cell*, 18(4), pp. 435–445. doi: 10.1016/j.molcel.2005.04.010.

Amé, J. C., Spenlehauer, C. and De Murcia, G. (2004) 'The PARP superfamily', *BioEssays*, 26(8), pp. 882–893. doi: 10.1002/bies.20085.

An, H. J. *et al.* (2007) 'Targeted RNA interference of phosphatidylinositol 3-kinase p110-beta induces apoptosis and proliferation arrest in endometrial carcinoma cells.', *The Journal of pathology*. England, 212(2), pp. 161–169. doi: 10.1002/path.2158.

Angulo, I. *et al.* (2013) 'Phosphoinositide 3-kinase δ gene mutation predisposes to respiratory infection and airway damage', *Science (New York, N.Y.)*, 342(6160), pp. 866–871. doi: 10.1126/science.1243292.

Barlow, C. A., Laishram, R. S. and Anderson, R. A. (2010) 'Nuclear Phosphoinositides: A Signaling Enigma Wrapped in a Compartmental Conundrum', *Trends in cell biology*, 20(1), p. 25. doi: 10.1016/j.tcb.2009.09.009.

Benistant, C., Chapuis, H. and Roche, S. (2000) 'A specific function for phosphatidylinositol 3-kinase alpha (p85alpha-p110alpha) in cell survival and for phosphatidylinositol 3-kinase beta (p85alpha-p110beta) in de novo DNA synthesis of human colon carcinoma cells.', *Oncogene*. England, 19(44), pp. 5083–5090. doi: 10.1038/sj.onc.1203871.

Berenjeno, I. M. *et al.* (2012) 'Both p110α and p110β isoforms of PI3K can modulate the impact of loss-of-function of the PTEN tumour suppressor', *Biochemical Journal*, 442(1), pp. 151–159. doi: 10.1042/BJ20111741.

Bi, L. *et al.* (1999) 'Proliferative defect and embryonic lethality in mice homozygous for a deletion in the p110alpha subunit of phosphoinositide 3-kinase.', *The Journal of biological chemistry*, 274(16), pp. 10963–8. doi: 10.1074/JBC.274.16.10963.

Bi, L. *et al.* (2002) 'Early embryonic lethality in mice deficient in the p110β catalytic subunit of PI 3-kinase', *Mammalian Genome*, 13(3), pp. 169–172. doi: 10.1007/s00335-001-2123-x.

Blind, R. D. *et al.* (2014) 'The signaling phospholipid PIP_3 creates a new interaction surface on the nuclear receptor SF-1', *Proceedings of the National Academy of Sciences*, 111(42), pp. 15054–15059. doi: 10.1073/pnas.1416740111.

Blind, R. D., Suzawa, M. and Ingraham, H. A. (2012) 'Direct modification and regulation of a nuclear receptor-PIP(2) complex by the nuclear inositol-lipid kinase IPMK', *Science Signaling*, 5(229), pp. ra44-ra44. doi: 10.1126/scisignal.2003111.

Boamah, E. K. *et al.* (2012) 'Poly(ADP-Ribose) polymerase 1 (PARP-1) regulates ribosomal biogenesis in Drosophila nucleoli.', *PLoS genetics*. United States, 8(1), p. e1002442. doi: 10.1371/journal.pgen.1002442.

Bokhman, J. V (1983) 'Two pathogenetic types of endometrial carcinoma.', *Gynecologic oncology*. United States, 15(1), pp. 10–17.

Boronenkov, I. V *et al.* (1998) 'Phosphoinositide signaling pathways in nuclei are associated with nuclear speckles containing pre-mRNA processing factors.', *Molecular biology of the cell*.

United States, 9(12), pp. 3547–3560.

Cancer Research UK (no date) *Uterine cancer statistics*. Available at: http://www.cancerresearchuk.org/health-professional/cancer-statistics/statistics-by-cancer-type/uterine-cancer#heading-Zero (Accessed: 4 May 2018).

Chakrabarti, R. *et al.* (2015) 'Phosphatidylinositol-4-phosphate 5-Kinase 1alpha Modulates Ribosomal RNA Gene Silencing through Its Interaction with Histone H3 Lysine 9 Trimethylation and Heterochromatin Protein HP1-alpha.', *The Journal of biological chemistry*. United States, 290(34), pp. 20893–20903. doi: 10.1074/jbc.M114.633727.

Chambon, P., Weill, J. D. and Mandel, P. (1963) 'Nicotinamide mononucleotide activation of new DNA-dependent polyadenylic acid synthesizing nuclear enzyme.', *Biochemical and biophysical research communications*. United States, 11, pp. 39–43.

Chang, C. Y.-Y. *et al.* (2016) 'Up-regulation of ribosome biogenesis by MIR196A2 genetic variation promotes endometriosis development and progression.', *Oncotarget*, 7(47), pp. 76713–76725. doi: 10.18632/oncotarget.11536.

Cocco, L. *et al.* (1987) 'Synthesis of polyphosphoinositides in nuclei of Friend cells. Evidence for polyphosphoinositide metabolism inside the nucleus which changes with cell differentiation', *Biochem J*, 248(3), pp. 765–770. doi: 10.1042/bj2480765.

Cully, M. *et al.* (2006) 'Beyond PTEN mutations: The PI3K pathway as an integrator of multiple inputs during tumorigenesis', *Nature Reviews Cancer*, 6(3), pp. 184–192. doi: 10.1038/nrc1819.

D'Amours, D. *et al.* (1999) 'Poly(ADP-ribosyl)ation reactions in the regulation of nuclear functions.', *Biochemical Journal*, 342(Pt 2), pp. 249–268. Available at: http://www.ncbi.nlm.nih.gov/pmc/articles/PMC1220459/.

Davis, W. J., Lehmann, P. Z. and Li, W. (2015) 'Nuclear PI3K signaling in cell growth and tumorigenesis', *Frontiers in Cell and Developmental Biology*, 3(April), pp. 1–14. doi: 10.3389/fcell.2015.00024.

Dbouk, H. A. *et al.* (2013) 'Characterization of a tumor-associated activating mutation of the p110beta PI 3-kinase.', *PloS one*. United States, 8(5), p. e63833. doi: 10.1371/journal.pone.0063833.

Dedes, K. J. *et al.* (2010) 'PTEN deficiency in endometrioid endometrial adenocarcinomas predicts sensitivity to PARP inhibitors.', *Science translational medicine*. United States, 2(53), p. 53ra75. doi: 10.1126/scitranslmed.3001538.

Derenzini, M., Montanaro, L. and Trere, D. (2017) 'Ribosome biogenesis and cancer.', *Acta histochemica*. Germany, 119(3), pp. 190–197. doi: 10.1016/j.acthis.2017.01.009.

Dou, Z. *et al.* (2013) 'Class IA PI3K p110β Subunit Promotes Autophagy through Rab5 Small GTPase in Response to Growth Factor Limitation', *Molecular Cell*. Elsevier Inc., 50(1), pp. 29–42. doi: 10.1016/j.molcel.2013.01.022.

Drakas, R., Tu, X. and Baserga, R. (2004) 'Control of cell size through phosphorylation of upstream binding factor 1 by nuclear phosphatidylinositol 3-kinase.', *Proceedings of the National Academy of Sciences of the United States of America*, 101(25), pp. 9272–6. doi: 10.1073/pnas.0403328101.

Edgar, K. A. *et al.* (2010) 'Isoform-specific phosphoinositide 3-kinase inhibitors exert distinct effects in solid tumors.', *Cancer research*. United States, 70(3), pp. 1164–1172. doi: 10.1158/0008-5472.CAN-09-2525.

Ehm, P. *et al.* (2015) 'The tumor suppressor SHIP1 colocalizes in nucleolar cavities with p53 and components of PML nuclear bodies.', *Nucleus (Austin, Tex.)*. United States, 6(2), pp. 154–164. doi: 10.1080/19491034.2015.1022701.

Evans-Metcalf, E. R. *et al.* (1998) 'Profile of women 45 years of age and younger with endometrial cancer.', *Obstetrics and gynecology*. United States, 91(3), pp. 349–354.

Falasca, M. and Maffucci, T. (2007) 'Role of class II phosphoinositide 3-kinase in cell signalling', *Biochemical Society Transactions*, 35(2), pp. 211–214. doi: 10.1042/BST0350211.

Farley, K. I. *et al.* (2015) 'Determinants of mammalian nucleolar architecture.', *Chromosoma*. Austria, 124(3), pp. 323–331. doi: 10.1007/s00412-015-0507-z.

Farmer, H. *et al.* (2005) 'Targeting the DNA repair defect in BRCA mutant cells as a therapeutic strategy.', *Nature*. England, 434(7035), pp. 917–921. doi: 10.1038/nature03445.

Ferlay, J. *et al.* (2015) 'Cancer incidence and mortality worldwide: sources, methods and major patterns in GLOBOCAN 2012.', *International journal of cancer*. United States, 136(5), pp. E359-86. doi: 10.1002/ijc.29210.

Gellersen, B., Brosens, I. A. and Brosens, J. J. (2007) 'Decidualization of the human endometrium: mechanisms, functions, and clinical perspectives.', *Seminars in reproductive medicine*. United States, 25(6), pp. 445–453. doi: 10.1055/s-2007-991042.

Ghetti, A. *et al.* (1992) 'hnRNP I, the polypyrimidine tract-binding protein: distinct nuclear localization and association with hnRNAs.', *Nucleic Acids Research*, 20(14), pp. 3671–3678. Available at: http://www.ncbi.nlm.nih.gov/pmc/articles/PMC334017/.

Gibbs, C. S. and Zoller, M. J. (1991) 'Rational scanning mutagenesis of a protein kinase identifies functional regions involved in catalysis and substrate interactions', *Journal of Biological Chemistry*, 266(14), pp. 8923–8931.

Ginisty, H. *et al.* (1999) 'Structure and functions of nucleolin.', *Journal of Cell Science*, 112 (Pt 6, pp. 761–772. doi: 10.1093/emboj/17.5.1476.

Gruenbaum, Y. and Foisner, R. (2015) 'Lamins: Nuclear Intermediate Filament Proteins with Fundamental Functions in Nuclear Mechanics and Genome Regulation', *Annual Review of Biochemistry*, 84(1), pp. 131–164. doi: 10.1146/annurev-biochem-060614-034115.

Hadjiolov, A. (1985) 'The Nucleolus and Ribosome Biogenesis', *Cell Biology Monographs*, pp. 1–263. doi: 10.1007/s13398-014-0173-7.2.

Hamann, B. L. and Blind, R. D. (2018) 'Nuclear phosphoinositide regulation of chromatin.', *Journal of cellular physiology*. United States, 233(1), pp. 107–123. doi: 10.1002/jcp.25886.

Hammond, G. R. V and Balla, T. (2015) 'Polyphosphoinositide binding domains: Key to inositol lipid biology.', *Biochimica et biophysica acta*. Netherlands, 1851(6), pp. 746–758. doi: 10.1016/j.bbalip.2015.02.013.

Hassa, P. O. *et al.* (2005) 'Acetylation of poly(ADP-ribose) polymerase-1 by p300/CREB-binding protein regulates coactivation of NF-κB-dependent transcription', *Journal of*

Biological Chemistry, 280(49), pp. 40450–40464. doi: 10.1074/jbc.M507553200.

Hassa, P. O. and Hottiger, M. O. (2008) 'The diverse biological roles of mammalian PARPS, a small but powerful family of poly-ADP-ribose polymerases.', *Frontiers in bioscience : a journal and virtual library*. United States, 13, pp. 3046–3082.

Hu, Y., Liu, Z. and Ye, K. (2005) 'Phosphoinositol lipids bind to phosphatidylinositol 3 (PI3)-kinase enhancer GTPase and mediate its stimulatory effect on PI3-kinase and Akt signalings.', *Proceedings of the National Academy of Sciences of the United States of America*. United States, 102(46), pp. 16853–16858. doi: 10.1073/pnas.0507365102.

Huang, C. *et al.* (2013) 'Nuclear Export Signal-Interacting Protein Forms Complexes with Lamin A/C-Nups To Mediate the CRM1-Independent Nuclear Export of Large Hepatitis Delta Antigen', *Journal of Virology*. 1752 N St., N.W., Washington, DC: American Society for Microbiology, 87(3), pp. 1596–1604. doi: 10.1128/JVI.02357-12.

Ibrahim, Y. H. *et al.* (2012) 'PI3K inhibition impairs BRCA1/2 expression and sensitizes BRCA-proficient triple-negative breast cancer to PARP inhibition.', *Cancer discovery*. United States, 2(11), pp. 1036–1047. doi: 10.1158/2159-8290.CD-11-0348.

Jamieson, S. *et al.* (2011) 'A drug targeting only p110alpha can block phosphoinositide 3-kinase signalling and tumour growth in certain cell types.', *The Biochemical journal*. England, 438(1), pp. 53–62. doi: 10.1042/BJ20110502.

Jao, C. Y. and Salic, A. (2008) 'Exploring RNA transcription and turnover in vivo by using click chemistry.', *Proceedings of the National Academy of Sciences of the United States of America*. United States, 105(41), pp. 15779–15784. doi: 10.1073/pnas.0808480105.

Jean, S. and Kiger, A. A. (2014) 'Classes of phosphoinositide 3-kinases at a glance', *Journal of Cell Science*. Bidder Building, 140 Cowley Road, Cambridge, CB4 0DL, UK, pp. 923–928. doi: 10.1242/jcs.093773.

Jia, S. *et al.* (2008) 'Kinase-dependent and -independent functions of the p110β phosphoinositide-3-kinase in cell growth, metabolic regulation and oncogenic transformation', *Nature*, 454(7205), pp. 776–779. doi: 10.1038/nature07091.

Kakuk, A. *et al.* (2006) 'Nucleolar localization of phosphatidylinositol 4-kinase PI4K230 in various mammalian cells.', *Cytometry. Part A : the journal of the International Society for Analytical Cytology*. United States, 69(12), pp. 1174–1183. doi: 10.1002/cyto.a.20347.

Kakuk, A. *et al.* (2008) 'Nuclear and nucleolar localization signals and their targeting function in phosphatidylinositol 4-kinase PI4K230.', *Experimental cell research*. United States, 314(13), pp. 2376–2388. doi: 10.1016/j.yexcr.2008.05.006.

Kandoth, C. *et al.* (2013) 'Integrated genomic characterization of endometrial carcinoma.', *Nature*. England, 497(7447), pp. 67–73. doi: 10.1038/nature12113.

Kang, S. *et al.* (2006) 'Oncogenic transformation induced by the p110beta, -gamma, and -delta isoforms of class I phosphoinositide 3-kinase.', *Proceedings of the National Academy of Sciences of the United States of America*, 103(5), pp. 1289–94. doi: 10.1073/pnas.0510772103.

Karlsson, T. *et al.* (2016) 'A polybasic motif in ErbB3-binding protein 1 (EBP1) has key functions in nucleolar localization and polyphosphoinositide interaction', *Biochemical Journal*, 473(14), pp. 2033–2047. doi: 10.1042/BCJ20160274.

Karlsson, T. *et al.* (2017) 'Endometrial cancer cells exhibit high expression of p110beta and its selective inhibition induces variable responses on PI3K signaling, cell survival and proliferation.', *Oncotarget*. United States, 8(3), pp. 3881–3894. doi: 10.18632/oncotarget.13989.

Kim, M. Y., Zhang, T. and Kraus, W. L. (2005) 'Poly (ADP-ribosyl) ation by PARP-1:PAR-laying'NAD into a nuclear signal', *Genes & development*, 19(17), pp. 1951–1967. doi: 10.1101/gad.1331805.ity.

Koppensteiner, R. *et al.* (2014) 'Effect of MRE11 loss on PARP-inhibitor sensitivity in endometrial cancer in vitro.', *PloS one*. United States, 9(6), p. e100041. doi: 10.1371/journal.pone.0100041.

Kozera, B. and Rapacz, M. (2013) 'Reference genes in real-time PCR', *Journal of Applied Genetics*. Berlin/Heidelberg: Springer Berlin Heidelberg, 54(4), pp. 391–406. doi: 10.1007/s13353-013-0173-x.

Krzystek-Korpacka, M. *et al.* (2016) 'Serum availability affects expression of common house-keeping genes in colon adenocarcinoma cell lines: implications for quantitative real-time PCR studies', *Cytotechnology*. Springer Netherlands, 68(6), pp. 2503–2517. doi: 10.1007/s10616-016-9971-4.

Kumar, A. *et al.* (2011) 'Nuclear but Not Cytosolic Phosphoinositide 3-Kinase Beta Has an Essential Function in Cell Survival', *Molecular and Cellular Biology*, 31(10), pp. 2122–2133. doi: 10.1128/MCB.01313-10.

Kumar, A., Fernandez-Capetillo, O. and Carrera, A. C. (2010) 'Nuclear phosphoinositide 3-kinase controls double-strand break DNA repair', *Proceedings of the National Academy of Sciences*, 107(16), pp. 7491–7496. doi: 10.1073/pnas.0914242107.

Kumar, N. *et al.* (2004) 'Association of Villin with Phosphatidylinositol 4,5-Bisphosphate Regulates the Actin Cytoskeleton', *Journal of Biological Chemistry*, 279(4), pp. 3096–3110. doi: 10.1074/jbc.M308878200.

Kwon, H. and Green, M. R. (1994) 'The RNA polymerase I transcription factor, upstream binding factor, interacts directly with the TATA box-binding protein.', *The Journal of biological chemistry*. United States, 269(48), pp. 30140–30146.

Kwon, I.-S. *et al.* (2010) 'PI(3,4,5)P3 regulates the interaction between Akt and B23 in the nucleus', *BMB reports*, 43(2), pp. 127–132. Available at: http://citeseerx.ist.psu.edu/viewdoc/download?doi=10.1.1.915.3308&rep=rep1&type=pdf (Accessed: 21 May 2018).

Lam, Y. W. and Lamond, A. I. (2006) 'Isolation of Nucleoli', in *Cell Biology*. Elsevier, pp. 103–107. doi: 10.1016/B978-012164730-8/50087-3.

Legartova, S. *et al.* (2014) 'Nuclear structures surrounding internal lamin invaginations.', *Journal of cellular biochemistry*. United States, 115(3), pp. 476–487. doi: 10.1002/jcb.24681.

Lemmon, M. A. (2003) 'Phosphoinositide recognition domains.', *Traffic (Copenhagen, Denmark)*. England, 4(4), pp. 201–213.

Lewis, A. E. *et al.* (2011) 'Identification of Nuclear Phosphatidylinositol 4,5-Bisphosphate-Interacting Proteins by Neomycin Extraction', *Molecular & Cellular Proteomics*, 10(2), p.

M110.003376. doi: 10.1074/mcp.M110.003376.

Li, J. *et al.* (1997) 'PTEN, a putative protein tyrosine phosphatase gene mutated in human brain, breast, and prostate cancer.', *Science (New York, N.Y.)*. United States, 275(5308), pp. 1943–1947.

Li, L., Dong, M. and Wang, X.-G. (2016) 'The Implication and Significance of Beta 2 Microglobulin: A Conservative Multifunctional Regulator', *Chinese Medical Journal*. India: Medknow Publications & Media Pvt Ltd, 129(4), pp. 448–455. doi: 10.4103/0366-6999.176084.

Li, P. *et al.* (2014) 'Identification of nucleolus-localized PTEN and its function in regulating ribosome biogenesis.', *Molecular biology reports*. Netherlands, 41(10), pp. 6383–6390. doi: 10.1007/s11033-014-3518-6.

Liang, H. *et al.* (2017) 'PTENβ is an alternatively translated isoform of PTEN that regulates rDNA transcription', *Nature Communications*. Nature Publishing Group, 8, pp. 1–14. doi: 10.1038/ncomms14771.

Lindsay, Y. *et al.* (2006) 'Localization of agonist-sensitive PtdIns(3,4,5)P3 reveals a nuclear pool that is insensitive to PTEN expression', *Journal of Cell Science*, 119(24), pp. 5160–5168. doi: 10.1242/jcs.000133.

Lizotte, E. *et al.* (2005) 'Isolation and characterization of subcellular protein fractions from mouse heart.', *Analytical biochemistry*. United States, 345(1), pp. 47–54. doi: 10.1016/j.ab.2005.07.001.

Maehama, T. and Dixon, J. E. (1998) 'The tumor suppressor, PTEN/MMAC1, dephosphorylates the lipid second messenger, phosphatidylinositol 3,4,5-trisphosphate.', *The Journal of biological chemistry*. United States, 273(22), pp. 13375–13378.

Marques, M. *et al.* (2008) 'Phosphoinositide 3-Kinases p110 and p110 Regulate Cell Cycle Entry, Exhibiting Distinct Activation Kinetics in G1 Phase', *Molecular and Cellular Biology*, 28(8), pp. 2803–2814. doi: 10.1128/MCB.01786-07.

Marques, M. *et al.* (2009) 'Specific function of phosphoinositide 3-kinase beta in the control of DNA replication.', *Proceedings of the National Academy of Sciences of the United States of America*, 106(18), pp. 7525–30. doi: 10.1073/pnas.0812000106.

Martin, T. F. (1998) 'Phosphoinositide lipids as signaling molecules: common themes for signal transduction, cytoskeletal regulation, and membrane trafficking.', *Annual review of cell and developmental biology*. United States, 14, pp. 231–264. doi: 10.1146/annurev.cellbio.14.1.231.

Mateo, J. *et al.* (2017) 'A First-Time-in-Human Study of GSK2636771, a Phosphoinositide 3 Kinase Beta-Selective Inhibitor, in Patients with Advanced Solid Tumors.', *Clinical cancer research : an official journal of the American Association for Cancer Research*. United States, 23(19), pp. 5981–5992. doi: 10.1158/1078-0432.CCR-17-0725.

Matulonis, U. *et al.* (2015) 'Phase II study of the PI3K inhibitor pilaralisib (SAR245408; XL147) in patients with advanced or recurrent endometrial carcinoma.', *Gynecologic oncology*. United States, 136(2), pp. 246–253. doi: 10.1016/j.ygyno.2014.12.019.

Mazloumi Gavgani, F., Lewis, A. E. and Aasland, R. (2017) *Nucleolar roles of the PI3K*

pathway in cancer and differentiation. ISBN: 978-82-308-3866-2

McStay, B. (2016) 'Nucleolar organizer regions: genomic "dark matter" requiring illumination.', *Genes & development*. United States, 30(14), pp. 1598–1610. doi: 10.1101/gad.283838.116.

Meder, V. S. *et al.* (2005) 'PARP-1 and PARP-2 interact with nucleophosmin/B23 and accumulate in transcriptionally active nucleoli.', *Journal of cell science*. England, 118(Pt 1), pp. 211–222. doi: 10.1242/jcs.01606.

Van Meer, G., Voelker, D. R. and Feigenson, G. W. (2008) 'Membrane lipids: Where they are and how they behave', *Nature Reviews Molecular Cell Biology*, 9(2), pp. 112–124. doi: 10.1038/nrm2330.

Misteli, T. (2001) 'The concept of self-organization in cellular architecture', *Journal of Cell Biology*, 155(2), pp. 181–185. doi: 10.1083/jcb.200108110.

Moxley, K. M. and McMeekin, D. S. (2010) 'Endometrial Carcinoma: A Review of Chemotherapy, Drug Resistance, and the Search for New Agents', *The Oncologist*, 15(10), pp. 1026–1033. doi: 10.1634/theoncologist.2010-0087.

Murali, R., Soslow, R. A. and Weigelt, B. (2014) 'Classification of endometrial carcinoma: More than two types', *The Lancet Oncology*. Elsevier Ltd, 15(7), pp. e268–e278. doi: 10.1016/S1470-2045(13)70591-6.

Murano, K. *et al.* (2008) 'Transcription Regulation of the rRNA Gene by a Multifunctional Nucleolar Protein, B23/Nucleophosmin, through Its Histone Chaperone Activity', *Molecular and Cellular Biology*, 28(10), pp. 3114–3126. doi: 10.1128/MCB.02078-07.

Nemeth, A. and Langst, G. (2011) 'Genome organization in and around the nucleolus.', *Trends in genetics : TIG*. England, 27(4), pp. 149–156. doi: 10.1016/j.tig.2011.01.002.

Neri, L. M. *et al.* (1999) 'Increase in nuclear phosphatidylinositol 3-kinase activity and phosphatidylinositol (3,4,5) trisphosphate synthesis precede PKC-ζ translocation to the nucleus of NGF-treated PC12 cells', *FASEB Journal*, 13(15), pp. 2299–2310. Available at: http://www.scopus.com/inward/record.url?eid=2-s2.0-0032797276&partnerID=40&md5=68376e2f41c17d14af8dd0b730610d18%5Cnhttp://www.scopus.com/record/display.url?eid=2-s2.0-0032797276&origin=inward&txGid=IsyL4GjRVFCFFWSO0QUu_Ac%3A9.

Neri, L. M. *et al.* (2002) 'The nuclear phosphoinositide 3-kinase/AKT pathway: a new second messenger system.', *Biochimica et biophysica acta*. Netherlands, 1584(2–3), pp. 73–80.

Nguyen, L. X. T. and Mitchell, B. S. (2013) 'Akt activation enhances ribosomal RNA synthesis through casein kinase II and TIF-IA', *Proceedings of the National Academy of Sciences*, 110(51), pp. 20681–20686. doi: 10.1073/pnas.1313097110.

Ni, J. *et al.* (2012) 'Functional characterization of an isoform-selective inhibitor of PI3K-p110β as a potential anti-cancer agent', *Cancer Discovery*, 5(4), pp. 425–433. doi: 10.1158/2159-8290.CD-12-0003.

Nofrini, V., Di Giacomo, D. and Mecucci, C. (2016) 'Nucleoporin genes in human diseases', *European Journal of Human Genetics*. Nature Publishing Group, 24(10), pp. 1388–1395. doi: 10.1038/ejhg.2016.25.

Ogawa, L. M. and Baserga, S. J. (2017) ‘Crosstalk between the nucleolus and the DNA damage response.’, *Molecular bioSystems*. England, 13(3), pp. 443–455. doi: 10.1039/c6mb00740f.

Okada, M., Jang, S.-W. and Ye, K. (2008) ‘Akt phosphorylation and nuclear phosphoinositide association mediate mRNA export and cell proliferation activities by ALY.’, *Proceedings of the National Academy of Sciences of the United States of America*. United States, 105(25), pp. 8649–8654. doi: 10.1073/pnas.0802533105.

Okkenhaug, K. (2013) ‘Signaling by the phosphoinositide 3-kinase family in immune cells.’, *Annual review of immunology*. United States, 31, pp. 675–704. doi: 10.1146/annurev-immunol-032712-095946.

Onstad, M. A., Schmandt, R. E. and Lu, K. H. (2016) ‘Addressing the Role of Obesity in Endometrial Cancer Risk, Prevention, and Treatment’, *Journal of Clinical Oncology*. American Society of Clinical Oncology, 34(35), pp. 4225–4230. doi: 10.1200/JCO.2016.69.4638.

Osborne, S. L. *et al.* (2001) ‘Nuclear PtdIns(4,5)P2 assembles in a mitotically regulated particle involved in pre-mRNA splicing.’, *Journal of cell science*. England, 114(Pt 13), pp. 2501–2511.

Di Paolo, G. and De Camilli, P. (2006) ‘Phosphoinositides in cell regulation and membrane dynamics.’, *Nature*. England, 443(7112), pp. 651–657. doi: 10.1038/nature05185.

Pazarentzos, E. *et al.* (2016) ‘Oncogenic activation of the PI3-kinase p110β isoform via the tumor-derived PIK3CβD1067Vkinase domain mutation’, *Oncogene*. Nature Publishing Group, 35(9), pp. 1198–1205. doi: 10.1038/onc.2015.173.

Pederson, T. (2011) ‘The nucleolus’, *Cold Spring Harbor Perspectives in Biology*, 3(3), pp. 1–15. doi: 10.1101/cshperspect.a000638.

Pollock, C. and Huang, S. (2010) ‘The Perinucleolar Compartment’, *Cold Spring Harbor Perspectives in Biology*. Cold Spring Harbor Laboratory Press, 2(2), p. a000679. doi: 10.1101/cshperspect.a000679.

Posor, Y. *et al.* (2013) ‘Spatiotemporal control of endocytosis by phosphatidylinositol-3,4-bisphosphate.’, *Nature*. England, 499(7457), pp. 233–237. doi: 10.1038/nature12360.

Resnick, A. C. *et al.* (2005) ‘Inositol polyphosphate multikinase is a nuclear PI3-kinase with transcriptional regulatory activity.’, *Proceedings of the National Academy of Sciences of the United States of America*. United States, 102(36), pp. 12783–12788. doi: 10.1073/pnas.0506184102.

Rozengurt, E., Soares, H. P. and Sinnet-Smith, J. (2014) ‘Suppression of feedback loops mediated by PI3K/mTOR induces multiple over-activation of compensatory pathways: an unintended consequence leading to drug resistance’, *Mol Cancer Therapy*, 13(11), pp. 2477–2488. doi: 10.1158/1535-7163.MCT-14-0330.

Samuels, Y. *et al.* (2004) ‘High Frequency of Mutations of the PIK3CA Gene in Human Cancers’, *Science*, 304(5670), p. 554. doi: 10.1126/science.1096502.

Sarbassov, D. D. *et al.* (2005) ‘Phosphorylation and Regulation of Akt / PKB by the Rictor-mTOR Complex’, *Science*, 307(5712), pp. 1098–1101. doi: 10.1126/science.1106148.

Sasaki, T. *et al.* (2009) ‘Mammalian phosphoinositide kinases and phosphatases’, *Progress in*

Lipid Research. Elsevier Ltd, 48(6), pp. 307–343. doi: 10.1016/j.plipres.2009.06.001.

Satoh, M. S. and Lindahl, T. (1992) 'Role of poly(ADP-ribose) formation in DNA repair.', *Nature*. England, 356(6367), pp. 356–358. doi: 10.1038/356356a0.

Savino, T. M. *et al.* (2001) 'Nucleolar assembly of the rRNA processing machinery in living cells.', *The Journal of cell biology*. United States, 153(5), pp. 1097–1110.

Schramp, M. *et al.* (2012) 'PIP kinases from the cell membrane to the nucleus.', *Sub-cellular biochemistry*. United States, 58, pp. 25–59. doi: 10.1007/978-94-007-3012-0_2.

Scott, M. S., Troshin, P. V and Barton, G. J. (2011) 'NoD: a Nucleolar localization sequence detector for eukaryotic and viral proteins.', *BMC bioinformatics*. England, 12, p. 317. doi: 10.1186/1471-2105-12-317.

Shah, Z. H. *et al.* (2013) 'Nuclear phosphoinositides and their impact on nuclear functions.', *The FEBS journal*. England, 280(24), pp. 6295–6310. doi: 10.1111/febs.12543.

Shen, Y. *et al.* (2013) 'BMN 673, a novel and highly potent PARP1/2 inhibitor for the treatment of human cancers with DNA repair deficiency.', *Clinical cancer research : an official journal of the American Association for Cancer Research*. United States, 19(18), pp. 5003–5015. doi: 10.1158/1078-0432.CCR-13-1391.

Smith, C. D. and Wells, W. W. (1983) 'Phosphorylation of rat liver nuclear envelopes. I. Characterization of in vitro protein phosphorylation', *The Journal of biological chemistry*, 258(15), pp. 9360–9367. Available at: http://www.ncbi.nlm.nih.gov/pubmed/6308004.

Sobol, M. *et al.* (2013) 'UBF complexes with phosphatidylinositol 4,5-bisphosphate in nucleolar organizer regions regardless of ongoing RNA polymerase I activity.', *Nucleus (Austin, Tex.)*. United States, 4(6), pp. 478–486. doi: 10.4161/nucl.27154.

Sobol, M. *et al.* (2018) 'Nuclear phosphatidylinositol 4,5-bisphosphate islets contribute to efficient RNA polymerase II-dependent transcription.', *Journal of cell science*. England, 131(8). doi: 10.1242/jcs.211094.

Stack, J. H. *et al.* (1995) 'Vesicle-mediated protein transport: regulatory interactions between the Vps15 protein kinase and the Vps34 PtdIns 3-kinase essential for protein sorting to the vacuole in yeast.', *The Journal of cell biology*. United States, 129(2), pp. 321–334.

Stelloo, E. *et al.* (2016) 'Improved Risk Assessment by Integrating Molecular and Clinicopathological Factors in Early-stage Endometrial Cancer-Combined Analysis of the PORTEC Cohorts.', *Clinical cancer research : an official journal of the American Association for Cancer Research*. United States, 22(16), pp. 4215–4224. doi: 10.1158/1078-0432.CCR-15-2878.

Tanaka, K. *et al.* (1999) 'Evidence that a phosphatidylinositol 3,4,5-trisphosphate-binding protein can function in nucleus.', *The Journal of biological chemistry*. United States, 274(7), pp. 3919–3922.

Tao, Z., Gao, P. and Liu, H. W. (2009) 'Identification of the ADP-ribosylation sites in the PARP-1 automodification domain: Analysis and implications', *Journal of the American Chemical Society*, 131(40), pp. 14258–14260. doi: 10.1021/ja906135d.

Thomson, E., Ferreira-Cerca, S. and Hurt, E. (2013) 'Eukaryotic ribosome biogenesis at a

glance.', *Journal of cell science*. England, 126(Pt 21), pp. 4815–4821. doi: 10.1242/jcs.111948.

Vadas, O. *et al.* (2011) 'Structural biology structural basis for activation and inhibition of class I phosphoinositide 3-kinases', *Science Signaling*, 4(195), pp. 1–13. doi: 10.1126/scisignal.2002165.

Vanhaesebroeck, B., Stephens, L. and Hawkins, P. (2012) 'PI3K signalling: The path to discovery and understanding', *Nature Reviews Molecular Cell Biology*. Nature Publishing Group, 13(3), pp. 195–203. doi: 10.1038/nrm3290.

Vanhaesebroeck, B. and Waterfield, M. D. (1999) 'Signaling by distinct classes of phosphoinositide 3-kinases', *Experimental Cell Research*, 253(1), pp. 239–254. doi: 10.1006/excr.1999.4701.

Viaud, J. *et al.* (2016) 'Phosphoinositides: Important lipids in the coordination of cell dynamics', *Biochimie*, 125, pp. 250–258. doi: 10.1016/j.biochi.2015.09.005.

Wang, X. and Jiang, X. (2008) 'PTEN: A default gate-keeping tumor suppressor with a versatile tail', *Cell Research*, 18(8), pp. 807–816. doi: 10.1038/cr.2008.83.

Wang, Z. and Cole, P. A. (2014) 'Catalytic Mechanisms and Regulation of Protein Kinases', *Methods in enzymology*, 548, pp. 1–21. doi: 10.1016/B978-0-12-397918-6.00001-X.

Wartko, P. *et al.* (2013) 'Recent changes in endometrial cancer trends among menopausal-age U.S. women.', *Cancer epidemiology*. Netherlands, 37(4), pp. 374–377. doi: 10.1016/j.canep.2013.03.008.

Wee, S. *et al.* (2008) 'PTEN-deficient cancers depend on PIK3CB', *Proceedings of the National Academy of Sciences*, 105(35), pp. 13057–13062. doi: 10.1073/pnas.0802655105.

Wickramasinghe, V. O. *et al.* (2013) 'Human inositol polyphosphate multikinase regulates transcript-selective nuclear mRNA export to preserve genome integrity.', *Molecular cell*. United States, 51(6), pp. 737–750. doi: 10.1016/j.molcel.2013.08.031.

Ye, K. *et al.* (2000) 'Pike. A nuclear gtpase that enhances PI3kinase activity and is regulated by protein 4.1N.', *Cell*. United States, 103(6), pp. 919–930.

Yildirim, S. *et al.* (2013) 'Involvement of phosphatidylinositol 4,5-bisphosphate in RNA polymerase I transcription', *Journal of Cell Science*, 126(12), pp. 2730–2739. doi: 10.1242/jcs.123661.

Yin, X. *et al.* (2012) 'Increased activation of the PI3K/AKT pathway compromises decidualization of stromal cells from endometriosis.', *The Journal of clinical endocrinology and metabolism*. United States, 97(1), pp. E35-43. doi: 10.1210/jc.2011-1527.

Zhang, L. *et al.* (2012) 'Phosphatidylinositol 4, 5 bisphosphate and the actin cytoskeleton.', *Sub-cellular biochemistry*. United States, 59, pp. 177–215. doi: 10.1007/978-94-007-3015-1_6.

Appendix

Amino acid sequence of GST-PARP1 fragments. The polybasic KR motifs are highlighted in blue, and the amino acid residues thought to be involved in PIP3 binding are highlighted in red:

Frag 1 (1-214) - MAESSDKLYR VEYAKSGRAS CKKCSESIPK DSLRMAIMVQ SPMFDGKVPH WYHFSCFWKV GHSIRHPDVE VDGFSELRWD DQQKVKKTAE AGGVTGKGQD GIGSKAEKTL GDFAAEYAKS NRSTCKGCME KIEKGQVRLS KKMVDPEKPQ LGMIDRWYHP GCFVKNREEL GFRPEYSASQ LKGFSLLATE DKEALKKQLP GVKSEGKRKG DEVD

Frag 2 (215-371) - GVDEVA KKKSKKEKDK DSKLEKALKA QNDLIWNIKD ELKKVCSTND LKELLIFNKQ QVPSGESAIL DRVADGMVFG ALLPCEECSG QLVFKSDAYY CTGDVTAWTK CMVKTQTPNR KEWVTPKEFR EISYLKKLKV KKQDRIFPPE TSASVAATPP P

Missing fragment 372-476

Frag 3 (477-524) - ILSP WGAEVKAEPV EVVAPRGKSG AALSKKSKGQ VKEEGINKSE KRMK

Frag 4 (525-656) - LTLKGG AAVDPDSGLE HSAHVLEKGG KVFSATLGLV DIVKGTNSYY KLQLLEDDKE NRYWIFRSWG RVGTVIGSNK LEQMPSKEDA IEHFMKLYEE KTGNAWHSKN FTKYPKKFYP LEIDYGQDEE AVKKLT

Frag 5 (657-1014) - VNPG TKSKLPKPVQ DLIKMIFDVE SMKKAMVEYE IDLQKMPLGK LSKRQIQAAY SILSEVQQAV SQGSSDSQIL DLSNRFYTLI PHDFGMKKPP LLNNADSVQA KVEMLDNLLD IEVAYSLLRG GSDDSSKDPI DVNYEKLKTD IKVVDRDSEE AEIIRKYVKN HATTHNAYD LEVIDIFKIE REGECQRYKP FKQLHNRRLL WHGSRTTNFA GILSQGLRIA PPEAPVTGYM FGKGIYFADM VSKSANYCHT SQGDPIGLIL LGEVALGNMY ELKHASHISK LPKGKHSVKG LGKTTPDPSA NISLDGVDVP LGTGISSGVN DTSLLYNEYI VYDIAQVNLK YLLKLKFNFK TSLW.